Genetic Fate Mapping Defines the Vascular Potential of Endocardial Cells in the Adult Heart

Juan Tang[1,2], Hui Zhang[1,2,3], Lingjuan He[1,2], Xiuzhen Huang[1,2], Yan Li[1,2], Wenjuan Pu[1,2], Wei Yu[1,2], Libo Zhang[1,2], Dongqing Cai[4], Kathy O. Lui[5], Bin Zhou[1-4]

[1]State Key Laboratory of Cell Biology, CAS Center for Excellence in Molecular Cell Science, Institute of Biochemistry and Cell Biology, Shanghai Institutes for Biological Sciences, University of Chinese Academy of Sciences, Chinese Academic of Sciences, Shanghai 200031, China; [2]Key Laboratory of Nutrition and Metabolism, Institute for Nutritional Sciences, Shanghai Institutes for Biological Sciences, University of Chinese Academy of sciences, Chinese Academy of Sciences, Shanghai, 200031, China; [3]School of Life Science and Technology, Shanghai Tech University, Shanghai, 201210, China; [4]Key Laboratory of Regenerative Medicine of Ministry of Education, Institute of Aging and Regenerative Medicine, Jinan University, Guangzhou, 510632 China, and; [5]Department of Chemical Pathology, Li Ka Shing Institute of Health Sciences, The Chinese University of Hong Kong, Prince of Wales Hospital, Shatin, Hong Kong SAR, 999077, China.

Running title: Endocardial Fate Mapping in the Adult Heart

Subject Terms:
Basic Science Research
Ischemia
Vascular Biology

Address correspondence to:
Dr. Bin Zhou
Shanghai Institutes for Biological Sciences
320 Yueyang Road
Shanghai, 200031
China
Tel: 86-21-54920974
zhoubin@sibs.ac.cn

In December 2017, the average time from submission to first decision for all original research papers submitted to *Circulation Research* was 13.60 days.

ABSTRACT

Rationale: Endocardium is the major source of coronary endothelial cells in the fetal and neonatal hearts. It remains unclear whether endocardium in the adult stage is also the main origin of neovascularization after cardiac injury.

Objective: To define the vascular potential of adult endocardium in homeostasis and after cardiac injuries by fate mapping studies.

Methods and Results: We generate an inducible adult endocardial Cre line (*Npr3-CreER*) and show that *Npr3-CreER* efficiently and specifically labels endocardial cells but not coronary blood vessels in the adult heart. The adult endocardial cells do not contribute to any vascular endothelial cells during cardiac homeostasis. To examine the formation of blood vessels from endocardium after injury, we generate four cardiac injury models with *Npr3-CreER* mice: myocardial infarction (MI), myocardial ischemia-reperfusion (IR), cryoinjury (CI), transverse aortic constriction (TAC). Lineage tracing experiments show that adult endocardium minimally contributes to coronary endothelial cells after MI. In the IR, CI or TAC models, adult endocardial cells do not give rise to any vascular endothelial cells, and they remain on the inner surface of myocardium that connects with lumen circulation. In the MI model, very few endocardial cells are trapped in the infarct zone of myocardium shortly after ligation of coronary artery, indicating the involvement of endocardial entrapment during blood vessels formation. When these adult endocardial cells are re-located and trapped in the infarcted myocardium by transplantation or myocardial constriction model, very few endocardial cells survive and gain vascular endothelial cell properties, and their contribution to neovascularization in the injured myocardium remains minimal.

Conclusions: Unlike its fetal or neonatal counterpart, adult endocardium naturally generates minimal, if any, coronary arteries or vascular endothelial cells during cardiac homeostasis or after injuries.

Keywords:
Coronary artery, adult endocardium, fate mapping, cardiac injury, animal model, cardiovascular disease.

Nonstandard Abbreviations and Acronyms:

MI	Myocardial infarction
IR	Myocardial ischemia reperfusion
CI	Cryoinjury
TAC	Transverse aortic constriction
ECs	Endothelial cells
MEndoT	Mesenchymal to endothelial transition
CoAs	Coronary arteries
PSSL	Purse-string suture-like model

INTRODUCTION

Coronary arteries are essential in the maintenance of normal heart function by supplying oxygenated blood to heart muscle. When coronary arteries are blocked, blood flow is reduced leading to hypoxia and subsequent death of cardiomyocytes. Neovascularization after myocardial infarction is, therefore, needed to prolong the survival of cardiomyocytes.[1, 2] Understanding how new coronary blood vessels form after injury offers important clinical insights into developing treatment of cardiovascular diseases and promoting cardiac regeneration.[3, 4]

In the developing heart, coronary blood vessels arise from three major sources including sinus venosus endocardial cells, ventricular endocardial cells and epicardial cells.[5–9] Sinus venosus endocardial cells migrate from epicardium and penetrate into myocardium to form coronary vessels at the early embryonic stage,[5] while ventricular endocardial cells contribute to coronary vessels in ventricular septum and inner myocardial wall at the embryonic and early neonatal stages.[10–12] Epicardial cells give rise to a subset of coronary vascular endothelial cells (ECs) and most of pericytes or smooth muscle cells through epithelial-to-mesenchymal transition.[8, 9, 13, 14] In the adult heart, sinus venosus is transformed into a specialized structure known as coronary sinus that collects blood from coronary veins.[15, 16] Epicardial cells in the adult heart react after injury through producing paracrine signals that promote angiogenesis. Nevertheless, lineage tracing data show that epicardial cells do not trans-differentiate into endothelial cells after injury.[17, 18] Recent studies suggest several new sources of neovascularization in the adult heart including resident cardiac fibroblasts and adult endocardial cells.[19, 20] In the adult heart, resident fibroblasts are mainly derived from the developing epicardiaum and endocardium.[18, 21, 22] Recent reports also show that these resident cardiac fibroblasts generate new coronary blood vessels through mesenchymal to endothelial transition (MEndoT).[19] However, fate-mapping studies employing new genetic lineage tracing tools demonstrate that cardiac fibroblasts remain in the fibroblast cell fate and do not trans-differentiate into new endothelial cells through MEndoT.[23] While endocardial cells contribute to a substantial number of coronary vascular endothelial cells in the fetal and neonatal stages,[7, 10] it remains elusive whether adult endocardial cells have the same potential to generate new coronary vessels. Recent reports suggest that, like their fetal or neonatal counterparts, the adult endocardial cells are an important source of endogenous arteriogenesis by contributing coronary endothelial cells to promote vascularization after myocardial infarction (MI).[20] Whether endocardial cells differentiate into coronary vessels in response to different cardiac injuries remain largely unexplored and incompletely understood, partly due to the lack of genetic tool that specifically targets endocardium in the adult stage.

Here we generated a genetic lineage tracing tool that efficiently and specifically labeled the adult endocardium. We found that adult endocardial cells literally did not contribute to new vascular endothelial cells during cardiac homeostasis and after injuries. When adult endocardium cells were re-positioned into the injured myocardium, very few of them survived after injury to gain vascular endothelial cell properties, and their contribution to neovascularization in the injured myocardium remained minimal.

METHODS

The authors will make all data, analytic methods and study materials available to other researchers. The authors declare that all data that support the findings of this study are available within the article and its Online Data Supplement. All animal protocols were approved by the Institutional Animal Care and Use Committee (IACUC) at the Institute for Nutritional Sciences and the Institute of Biochemistry and Cell Biology, Shanghai Institutes for Biological Sciences, Chinese Academy of Science. The *Npr3-CreER* mouse line was generated by Shanghai Biomodel Organism Co., Ltd. All data were presented as mean values ± SEM. Statistical comparisons between data sets were done by a two-side unpaired Student's *t* test for comparing differences between two groups. $^{*}P < 0.05$ was considered to be statistically significant. Detailed materials and methods are included in the Online Data Supplement.

RESULTS

Npr3-CreER labels endocardial cells but not coronary vessels.

To address if adult endocardial cells contribute to new coronary blood vessels, we need an inducible Cre mouse line that specifically targets the adult endocardium but not its fetal counterpart. Recently we have identified a new endocardial cell marker Npr3 and generated the *Npr3-CreER* knock-in mouse line for studying the origin of embryonic coronary vessels.[12] Since this CreER knock-in is a null allele for Npr3, *Npr3-CreER* mouse used in this study was heterozygous (one allele loss). To examine if the loss of one Npr3 gene allele causes any heart defect, we systematically compared cardiac function, tissue fibrosis, capillary density and cardiomyocyte cell size between *Npr3-CreER* heterozygous and littermate wild-type mice. We did not detect any morphological or functional cardiac defect in the *Npr3-CreER* mouse line (Online Figure IA-I).

To test if *Npr3-CreER* labels adult endocardial cells, we crossed it with reporter line *R26-tdTomato*.[24] Cre-loxP recombination removes transcriptional stop cassette, leading to expression of tdTomato in Npr3$^+$ cells. Since the genetic tracing marker is heritable and permanent,[25] all the descendants of Npr3$^+$ cells would also express tdTomato even if they differentiated into other cell lineages. We injected tamoxifen to adult *Npr3-CreER;R26-tdTomato* mice and collected hearts for analysis at 48 hours after induction. By whole-mount and sectional views of the *Npr3-CreER;R26-tdTomato* heart, we detected robust tdTomato$^+$ signals in both right and left atria (Figure 1A,B). These tdTomato$^+$ cells were located in the innermost lining of the ventricular wall, indicative of endocardium; and partially in the outmost lining of the ventricular wall, indicative of a subset of epicardium (Figure 1B). Immunostaining for tdTomato and endothelial cell marker PECAM on heart sections confirmed that tdTomato$^+$ cells were indeed endocardial endothelial cells (Figure 1C-E).

We also noticed that some tdTomato$^+$ cells located inside the ventricular wall rather than on the surface of inner myocardial wall (Figure 1B). Immunostaining for tdTomato and alpha smooth muscle actin (aSMA) showed that these tdTomato$^+$ tube-like structures were not coronary arteries (Figure 1F). Additionally, we co-stained the coronary vascular endothelial cell marker FABP4 with tdTomato, and found that these tdTomato$^+$ tube-like structures inside myocardium were not FABP4$^+$ coronary vessels (Figure 1G). In fact, they were endocardial tunnels but not coronary vessels, as the tube-like structures were likely due to the arbitrary orientation of section plane on the irregular surface of inner myocardium wrapped with endocardium. Immunostaining for VE-Cad, aSMA and FABP4 on serial sections of littermate non-transgenic mouse hearts confirmed the existence of endocardial tunnels in the wild-type mouse heart (Online Figure IJ).

We also quantified the percentage of tdTomato$^+$ cells among the endocardial cells and found that *Npr3-CreER* efficiently labeled endocardial cells in both atria, right and left ventricles (>90%) (Figure 1H). Taken together, these data demonstrated that *Npr3-CreER* specifically and efficiently labeled endocardial cells (Endo) but not coronary arteries or cardiac vascular endothelial cells in the adult heart (Figure 1I). *Npr3-CreER*-mediated endocardial tracing would be useful to address if endocardial cells generate vascular endothelial cells in the adult heart during homeostasis or after injuries.

Adult endocardial cells maintain the endocardial cell fate in homeostasis.

To understand if adult endocardial cells maintain the endocardial cell fate or may also generate new coronary vessels, we induced tamoxifen in *Npr3-CreER;R26-tdTomato* mice at week 4 and collected hearts for analysis at week 20 for young adult mouse and at week 62 for aged mice, respectively (Figure 2A). Whole heart fluorescence section of 20 weeks mouse hearts showed that tdTomato expression was enriched in the innermost layer and also in a subset of cells within the outermost layer of the heart, indicative of

endocardial cells and a subset of epicardial cells, respectively (Figure 2B). These tdTomato$^+$ cells expressed endothelial cell marker PECAM lining the innermost layer of the heart, confirming the endocardial cell identity (Figure 2C). In the young adult hearts, a few tdTomato$^+$ tube-like structures were also detected inside the myocardium of ventricular wall (asterisk, Figure 2C). We interpreted them as component of the endocardium but less likely the coronary vessels for the following reasons. Immunostaining for FABP4 and tdTomato showed that tdTomato$^+$ tube-like structures were FABP4$^-$ (Figure 2D), indicating that they were not vascular endothelial cells. Moreover, the tube-like structures were usually large in diameter, but they were not coronary arteries (CoAs) as they lacked aSMA$^+$ smooth muscle cells (Figure 2E). Consistent with the results of young adult mice, endocardial cells did not generate new blood vessels in 62 weeks old mouse heart (Online Figure II). Furthermore, serial sections of the hearts showed that the tube-like structures in the myocardium were connected with chamber circulation (Online Figure III). In addition, we also injected the fluorescein dye, CellTracker Green CMFDA, into the heart chamber of *Npr3-CreER;R26-tdTomato* mice and detected CMFDA in the *Npr3-CreER* labeled endocardial cells (tdTomato$^+$), which located between the trabeculation grooves (Figure 2F).

Next, we isolated tdTomato$^+$ and tdTomato$^-$ endothelial cells from *Npr3-CreER;R26-tdTomato* hearts by flow cytometry and performed quantitative reverse-transcription PCR (*qRT-PCR*) to check expression of genes by endocardial and vascular endothelial cells (Figure 2G, Online Figure IV). While *Npr3* was highly enriched in tdTomato$^+$ ECs compared with tdTomato$^-$ ECs, expression level of *Fabp4* and *Apln* were significantly reduced in tdTomato$^+$ ECs compared with tdTomato$^-$ ECs. The universal endothelial cell marker *Cd31* was equally expressed in both populations (Figure 2H). Since *Npr3-CreER* labeled endocardium did not contribute to new coronary vessels in the adult stage, we used *Npr3-CreER* to label fetal endocardium that served as a positive control of the tracing system. We induced tamoxifen in *Npr3-CreER;R26-tdTomato* mice at E13.5 and collected postnatal hearts for analysis (Figure 2I). Consistent with the previous study,[10] labeled endocardial cells in the fetal stage mainly contributed to the coronary vessels of the inner myocardial wall (Figure 2I,J). These data demonstrated that fetal but not adult endocardial cells contributed to new vascular endothelial cells in the ventricular wall.

Adult endocardial cells contribute minimally to coronary vessels after cardiac injuries.

We next asked if adult endocardial cells respond to cardiac injuries and if the developmental program of embryonic endocardial cells can be re-capitulated in adults to generate new coronary blood vessels. We performed moderate and severe myocardial infarction (MI), respectively, on *Npr3-CreER;R26-tdTomato* hearts at week 6-8 and collected hearts 2-4 weeks following MI. In the moderate MI model, staining with whole-mount heart sections showed that tdTomato$^+$ cells were largely restricted to the innermost layer of the MI hearts (Figure 3A). Immunostaining for tdTomato and FABP4 showed no tdTomato labeled FABP4$^+$ cardiac vascular endothelial cells in the border and infarct regions of the MI hearts (Figure 3B-D). In the severe MI model, immunostaining for tdTomato and FABP4 on heart sections showed that there were very sparse tdTomato$^+$FABP4$^+$ cardiac vascular endothelial cells in the border region of the MI hearts (Online Figure VA-D). Quantification data showed that, in the border zone, 0.034 ± 0.010% of FABP4$^+$ cardiac vascular endothelial cells were tdTomato$^+$, while the efficiency of endocardial (Endo.) labeling remained as high as 90.67 ± 1.69% in the ventricular walls (Online Figure VE). We did not detect any FABP4$^+$tdTomato$^+$ cardiac vascular endothelial cells in the remote region of the MI hearts even though endocardial cells were efficiently labeled in that region (Online Figure VA-E). To exclude the possibility that these tdTomato$^+$ tube-like structures in the MI hearts were coronary arteries, we also performed immunostaining for aSMA and found that they were not aSMA$^+$ coronary arteries (Figure 3E-F; Online Figure VF). Moreover, immunostaining for PECAM and tdTomato on serial sections confirmed that the tdTomato$^+$ tube-like structures were connected with the chamber circulation (Online Figure VI), indicating that they were endocardial cells but not vascular endothelial cells.

Since endocardial cells hardly contributed to cardiac vascular endothelial cells after MI, we next generated vascular endothelial cell tracer *Apln-CreER* to test if pre-existing vessels mainly mediated neovascularization after injury. Unlike PECAM, Cdh5 or Tie2 genes that are expressed in both vascular and endocardial endothelial cells, Apln is specifically expressed in vascular endothelial cells but not endocardial cells.[6] By tamoxifen treatment after MI, we found that *Apln-CreER* labeled a significant number of endothelial cells compared with sham controls (Online Figure VIIA,B), indicating active sprouting angiogenesis marked by Apln.[26] To reveal the sources of the putative nascent vessels in injured myocardium, we used an alternative strategy that labeled pre-existing vessels by tamoxifen treatment before MI (Online Figure VIIC). We found that almost all vascular endothelial cells in the injured myocardium were tdTomato$^+$ (Online Figure VIID), indicating they were derived from pre-existing vessels labeled before MI. Quantification of the percentage of labeled vessels showed no significant difference between samples collected before and after MI (Online Figure VIIE). These data indicate that proliferation or expansion of pre-existing vessels mainly mediated neovascularization in injured myocardium. To distinguish newly formed vessels (nascent vessels) from those non-proliferating pre-existing vessels in the injured myocardium, we used EdU incorporation to mark the newly formed vessels (Online Figure VIIF). Immunostaining for tdTomato, EDU and FABP4 on MI heart sections showed robust endothelial cell proliferation in the injured myocardium but not in sham controls (Online Figure VIIG). This data showed that the newly formed vessels of injured myocardium were derived from pre-existing vessels labeled before injury, and also distinguished nascent vessel formation (EdU$^+$tdTomato$^+$FABP4$^+$) from the non-proliferating pre-existing vessels (EdU$^-$tdTomato$^+$FABP4$^+$). These studies demonstrated that pre-existing vessels proliferated to generate new blood vessels (nascent vessels) in the injured myocardium, and the results were in consistent with previous study that pre-existing vessels mainly mediated neovascularization after cardiac injury.[23]

In a parallel experiment, we also used a myocardial infarction-reperfusion (IR) model to address if endocardial cells regained the plasticity to generate vascular cells after injury. Our results showed that the tdTomato$^+$ cells were mainly located within the innermost layer, adopting an endocardail cell fate (Figure 3G). These tdTomato$^+$ cells did not differentiate into FABP4$^+$ cardiac vascular endothelial cells (Figure 3H), nor into endothelial cells of aSMA$^+$ coronary arteries (Figure 3I). These data suggest that endocardial cells contributed to very few coronary vessels after MI, but not to any coronary vessels after IR. The difference between the MI and IR model was the permanent ligation in MI but not in IR during experiments. We reasoned that ligation might cause regional distortion of myocardium that might lead to entrapment of some of the endocardium. We therefore performed cryo-injury (CI) to ablate coronary artery under epicardium without significant distortion of the myocardium underlying endocardium. We found that tdTomato$^+$ cells did not form cardiac vascular endothelial cells in the injured *Npr3-CreER;R26-tdTomato* myocardium (Online Figure VIII). These data indicate that endocardial cells did not contribute to neovascularization after ischemic injury. The very few coronary endothelial cells derived from endocardium after severe MI could be due to distortion of the myocardium during permanent coronary ligation.

Since endocardial cells were located in the inner myocardial wall, we asked if the tension from the chamber might remodel these endocardial cells to form new coronary vessels. By utilizing the transverse aortic constriction (TAC) model at week 8, we analyzed hearts 4 or 6 weeks after TAC. Immunostaining for PECAM and tdTomato showed that the tdTomato$^+$ cells were largely restricted to the innermost layer of the myocardium, adopting an endothelial cell fate (Figure 3J). Moreover, immunostaining on serial sections confirmed that the tdTomato$^+$PECAM$^+$ tube-like structures were indeed connected with chamber circulation (Online Figure IX), indicative of a non-vascular phenotype. Furthermore, co-staining FABP4 or aSMA with tdTomato confirmed that tdTomato$^+$ cells were not CoECs and not associated with coronary arteries (Figure 3K,L). As *Npr3-CreER* also labeled a subset of epicardial cells in addition to endocardial cells, we next used an epicardial driver *Wt1-CreER*[13] to test if the epicardium differentiates into vascular endothelial cells after injury. We found that epicardial cells hardly contributed to vascular endothelial cells in the injured myocardium after MI or IR (Online Figure X), which was consistent with previous studies.[17,

[18] Taken together, our results showed that adult endocardial cells contributed minimally to vascular endothelial cells after MI, and did not generate new vessels after IR or TAC injuries.

Relocated or trapped adult endocardial cells minimally contribute to neovascularization.

Entrapment of endocardial cells in the myocardium is observed during coronary vessel formation. Differentiation of endocardial to vascular endothelial cells is accompanied with trabecular coalescence and compaction at the late embryonic or early neonatal stage.[10] However, there is no further gross morphological change such as trabecular compaction in the adult heart. While endocardial cells remain on the surface of inner myocardial wall and communicate with chamber circulation, we asked if relocation of adult endocardial cells into myocardium could unlock their plasticity for vascular differentiation similar to their embryonic or neonatal counterparts. To recapitulate this differentiation program, we isolated adult endocardial cells and transplanted them into the myocardium of MI hearts (10^4 per heart, Figure 4A). We obtained heart samples at 3, 7 and 14 days after transplantation and examined their cell fates in the infarcted myocardium (Figure 4B). Immunostaining for tdTomato, PECAM or FABP4 showed that the endocardium-derived cells gained partial vascular endothelial cell properties (e.g. FABP4 expression) and capillary morphology (Figure 4C). Quantification of the percentage of tdTomato$^+$ cardiac vascular endothelial cells among the remaining transplanted tdTomato$^+$ cells revealed that most tdTomato$^+$ cells residing in the infarcted myocardium expressed FABP4. However, their contribution to injury-induced angiogenesis was minimal, as only ~0.3-0.4% vascular endothelial cells in the injured myocardium were endocardium-derived (Figure 4D). We also transplanted endocardial cells into the myocardium of normal hearts but was hardly able to find any tdTomato$^+$FABP4$^+$ cells remaining in the myocardium (Online Figure XI), suggesting that entrapment of endocardial cells in the myocardium was required but not sufficient to regain their vascular properties. The local environmental niche in the injured myocardium may promote survival and differentiation of endocardial cells to coronary vessels. Specifically, ischemia-induced hypoxia in the injured myocardium was demonstrated by immunostaining for hypoxyprobe (Online Figure XI). To ascertain if very few living tdTomato$^+$FABP4$^+$ endothelial cells of the infarcted myocardium were connected with circulation, we injected FITC-labeled BS1-lectin intravenously to label endothelial cells connected with the murine circulation.[27] We found that tdTomato$^+$ capillary endothelial cells were BS1-lectin positive (Figure 4E), indicating their incorporation into the vessels within the injured myocardium. These data suggest that endocardial cells have potential to contribute to coronary vascular endothelial cells, but their contribution was minimal for injury-induced neovascularization.

To further test if adult endocardial cells have potential to generate coronary vessels *in vivo*, we generated a purse-string suture-like model (PSSL) in which part of the left ventricular myocardium was distorted so that part of the endocardium was trapped and isolated from chamber circulation (Figure 4F). By Sirius Red staining, we confirmed severe injury in the distorted myocardium region (Figure 4G). Immunostaining for tdTomato and FABP4 on PSSL injured heart sections showed that a significant number of endocardium-derived cells (tdTomato$^+$) were FABP4$^+$ coronary vascular endothelial cells in the infarcted region (Figure 4H), indicating that the trapped endocardial cells gained some of the vascular cell properties after PSSL injury. In contrast, endocardial cells in the non-injured region did not differentiate into coronary vessels (Figure 4H). Interestingly, a subset of tdTomato$^+$ endothelial cells were coronary arteries in the border zone of the injured region (Figure 4I), suggesting that adult endocardial cells might have the potential to re-constitute part of the coronary artery. In spite of these positive observations, the contribution of endocardium-derived vascular cells (tdTomato$^+$) remained negligible and regional compared with the vast majority of the unlabeled coronary vessels in most regions (Figure 4H,I). Taken together, these data indicate that entrapped endocardium contributed minimally to injury-induced neovascularization in the adult heart.

DISCUSSION

Endocardial cells have been well studied during the cardiac cushion/valve development and trabecular formation.[28, 29] In addition to mesenchymal cells in cardiac cushion, endocardial cells have been recently found to contribute to multiple cell lineages including coronary endothelial cells, pericytes or smooth muscle cells, fibroblasts, adipocytes and cardiomyocytes.[5, 7, 21, 30, 31] Unraveling the endocardial plasticity and sources of coronary vessels could provide new insights into promotion of therapeutic neovascularization or cardiac regeneration in treatment of MI. In this study, we showed that while endocardial cells contributed to coronary ECs in the embryonic or neonatal stage, their vascular potential was significantly reduced in the adult stage. We did not find any formation of blood vessels from endocardium in the adult heart during homeostasis and aging. There were minimal, if any, blood vessels derived from adult endocardium after cardiac injuries including the MI, IR or TAC models. Our experimental data also supported that re-location of endocardial cells into the myocardium could be critical for regaining properties of vascular endothelial cells from endocardium. Entrapment and injury-induced environmental change such as hypoxia were required for unlocking the vascular potential of adult endocardial cells.

Previous study identified the endocardium as a new site of endogenous arteriogenesis and a source of new coronary endothelial cells to promote neovascularization after MI.[20] By genetic lineage tracing of arterial ECs using the connexin 40 (*Cx40*)-*CreER* line, it has been demonstrated that new $Cx40^+$ arterial ECs could arise adjacent to endocardium after injury and were not genetically labeled. They have been interpreted as derivatives of the endocardium.[20] While the new $Cx40^+$ ECs are not derived from pre-existing $Cx40^+$ arterial ECs, it lacks direct lineage tracing evidence that they indeed arise from endocardial cells, in spite of their physical location that they are adjacent to the endocardium. It is also likely that the pre-existing $Cx40^-$ capillary ECs (unlabeled by *Cx40-CreER*) form *de novo* arteries that begin to express Cx40 and recruit smooth muscle cells in injured myocardium. Our current study utilized a new genetic tool *Npr3-CreER* that specifically and efficiently labeled adult endocardial cells, providing a direct lineage tracing system for fate mapping of adult endocardial cells.

While adult endocardial cells do not generate new coronary ECs, their fetal counterparts contribute to a substantial number of coronary ECs in late embryonic and early neonatal stages.[10, 12] This raises an intriguing question as to what underlying mechanism drives the significant difference in the vascular potential of fetal and adult endocardial cells. It is possible that the intrinsic endocardial cell plasticity is significantly lost during postnatal heart growth and maturation. However, we showed that this is less likely as transplantation of adult endocardial cells into adult myocardium led to gaining of vascular endothelial cell properties, which happened to the surviving endocardial cells remained in the infarcted myocardium. Interestingly, formation of blood vessels from endocardium is closely associated with trabecular compaction during embryonic and early neonatal stages, indicating that trapping of endocardial cells into compacting trabecular myocardium might be critical for cell fate transition.[32, 33] Since trabecular myocardium resolves and is replaced by compact myocardium in the adult heart, endocardial cells lining the innermost of myocardium are not trapped deep into myocardium, nor do they migrate deep into myocardium in homeostasis and after injury. In this case, one of the efficient ways to generate new coronary ECs might be through self-expansion of pre-existing coronary ECs.[23] When endocardial cells were trapped in the myocardium in PSSL model (Figure 4J) or when they were transplanted into the infarcted myocardium, they begin to gain some vascular endothelial cell properties. However, their bulk number or relative contribution to neovascularization is minimal in the injured myocardium. Unlike its embryonic or neonatal counterpart, the formation of coronary vessels from endocardium did not take place naturally in the adult stage. Even if endocardial cells were transplanted into normal cardiac tissues, they did not incorporate into the host vasculature. Previous study suggests that hypoxia and VEGFA are critical for lineage conversion of endocardial cells to vascular endothelial cells.[10] It is likely that hypoxic condition after MI (Online Figure XIB) stimulated this lineage conversion so the endocardial cells were incorporated

into the host vasculature and became part of the functional vessels. We reasoned that the non-vascular endocardial cells in non-hypoxic myocardium might die or be removed from the host tissue, as they were not incorporated into the host vascular system. These data suggest that physical location and also local environmental niche could be critical in the formation of vascular endothelial cells. It is important to understand the molecular mechanisms that unlock the vascular potential of adult endocardium, such as hypoxia-VEGF signaling as suggested in the neonatal coronary vessel formation.[10] Further experiments are needed in the future to determine the signaling pathways controlling formation of blood vessels from endocardium during heart development and pathogenesis.

ACKNOWLEDGMENTS

We thank Shanghai Biomodel Organism Co., Ltd. for mouse generation; and Baojin Wu, Guoyuan Chen, Zhonghui Weng and Aimin Huang for animal husbandry. We also thank the technical help from Wei Bian, Tengfei Zhang and members of National Center for Protein Science Shanghai for assistance in microscopy, all other members in Zhou lab.

SOURCES OF FUNDING

This work was supported by the Strategic Priority Research Program of the Chinese Academy of Sciences (CAS, XDB19000000, XDA16020204), National Science Foundation of China (31730112, 91639302, 31625019, 81761138040，31571503, 31501172, 31601168, 31701292, 91749122), National key Research & Development Program of China (2016YFC1300600 and 2017YFC1001303), Youth Innovation Promotion Association of CAS (2015218, 2060299), Key Project of Frontier Sciences of CAS (QYZDB-SSW-SMC003), International Cooperation Fund of CAS, National Program for Support of Top-notch Young Professionals and Leading Talents, Shanghai Science and Technology Commission (17ZR1449600, 17ZR1449800), Shanghai Yangfan Project (16YF1413400) and Rising-Star Program (15QA1404300), China Postdoctoral Science Foundation (2017M621552, 2017M611634), National Postdoctoral Program for Innovative Talents (BX201700267), China Young Talents Lift Engineering (2017QNRC001), President Fund of Shanghai Institutes for Biological Sciences (SIBS), Astrazeneca, Boehringer Ingelheim, Sanofi-SIBS Fellowship, Royal Society-Newton Advanced Fellowship, Research Council of Hong Kong (04110515, 14111916, C4024-16W) and Health and Medical Research Fund (03140346, 04152566).

DISCLOSURES

None.

REFERENCES

1. Carmeliet P. Angiogenesis in life, disease and medicine. *Nature*. 2005;438:932-936.
2. Luttun A, Carmeliet P. De novo vasculogenesis in the heart. *Cardiovasc Res*. 2003;58:378-389.
3. Riley PR, Smart N. Vascularizing the heart. *Cardiovasc Res*. 2011;91:260-268.
4. Hodgkinson CP, Bareja A, Gomez JA, Dzau VJ. Emerging Concepts in Paracrine Mechanisms in Regenerative Cardiovascular Medicine and Biology. *Circ Res*. 2016;118:95-107.
5. Red-Horse K, Ueno H, Weissman IL, Krasnow MA. Coronary arteries form by developmental reprogramming of venous cells. *Nature*. 2010;464:549-553.
6. Tian X, Hu T, Zhang H, He L, Huang X, Liu Q, Yu W, He L, Yang Z, Zhang Z, Zhong TP, Yang X, Yang Z, Yan Y, Baldini A, Sun Y, Lu J, Schwartz RJ, Evans SM, Gittenberger-de Groot AC, Red-Horse K, Zhou B. Subepicardial endothelial cells invade the embryonic ventricle wall to form coronary arteries. *Cell Res*. 2013;23:1075-1090.
7. Wu B, Zhang Z, Lui W, Chen X, Wang Y, Chamberlain AA, Moreno-Rodriguez R, Markwald R, O?Rourke B, Sharp D, Zheng D, Lenz J, Baldwin H, Chang C-P, Zhou B. Endocardial Cells Form the Coronary Arteries by Angiogenesis through Myocardial-Endocardial VEGF Signaling. *Cell*. 2012;151:1083-1096.
8. Perez-Pomares JM, Phelps A, Sedmerova M, Carmona R, Gonzalez-Iriarte M, Munoz-Chapuli R, Wessels A. Experimental studies on the spatiotemporal expression of WT1 and RALDH2 in the embryonic avian heart: a model for the regulation of myocardial and valvuloseptal development by epicardially derived cells (EPDCs). *Dev Biol*. 2002;247:307-326.
9. Katz T, Singh M, Degenhardt K, Rivera-Feliciano J, Johnson R, Epstein J, Tabin C. Distinct Compartments of the Proepicardial Organ Give Rise to Coronary Vascular Endothelial Cells. *Developmental Cell*. 2012;22:639-650.
10. Tian X, Hu T, Zhang H, He L, Huang X, Liu Q, Yu W, He L, Yang Z, Yan Y, Yang X, Zhong TP, Pu WT, Zhou B. De novo formation of a distinct coronary vascular population in neonatal heart. *Science*. 2014;345:90-94.
11. Chen HI, Sharma B, Akerberg BN, Numi HJ, Kivela R, Saharinen P, Aghajanian H, McKay AS, Bogard PE, Chang AH, Jacobs AH, Epstein JA, Stankunas K, Alitalo K, Red-Horse K. The sinus venosus contributes to coronary vasculature through VEGFC-stimulated angiogenesis. *Development*. 2014;141:4500-4512.
12. Zhang H, Pu W, Li G, Huang X, He L, Tian X, Liu Q, Zhang L, Wu SM, Sucov HM, Zhou B. Endocardium Minimally Contributes to Coronary Endothelium in the Embryonic Ventricular Free Walls. *Circ Res*. 2016;118:1880-1893.
13. Zhou B, Ma Q, Rajagopal S, Wu SM, Domian I, Rivera-Feliciano J, Jiang D, von Gise A, Ikeda S, Chien KR, Pu WT. Epicardial progenitors contribute to the cardiomyocyte lineage in the developing heart. *Nature*. 2008;454:109-113.
14. Cano E, Carmona R, Ruiz-Villalba A, Rojas A, Chau YY, Wagner KD, Wagner N, Hastie ND, Munoz-Chapuli R, Perez-Pomares JM. Extracardiac septum transversum/proepicardial endothelial cells pattern embryonic coronary arterio-venous connections. *Proc Natl Acad Sci U S A*. 2016;113:656-661.
15. DeRuiter MC, Gittenberger-De Groot AC, Wenink AC, Poelmann RE, Mentink MM. In normal development pulmonary veins are connected to the sinus venosus segment in the left atrium. *Anat Rec*. 1995;243:84-92.
16. Anderson RH, Brown NA, Moorman AF. Development and structures of the venous pole of the heart. *Dev Dyn*. 2006;235:2-9.
17. Zhou B, Honor LB, He H, Ma Q, Oh JH, Butterfield C, Lin RZ, Melero-Martin JM, Dolmatova E, Duffy HS, Gise A, Zhou P, Hu YW, Wang G, Zhang B, Wang L, Hall JL, Moses MA, McGowan FX, Pu WT. Adult mouse epicardium modulates myocardial injury by secreting paracrine factors. *J Clin Invest*. 2011;121:1894-1904.
18. Moore-Morris T, Guimaraes-Camboa N, Banerjee I, Zambon AC, Kisseleva T, Velayoudon A, Stallcup WB, Gu Y, Dalton ND, Cedenilla M, Gomez-Amaro R, Zhou B, Brenner DA, Peterson KL, Chen

J, Evans SM. Resident fibroblast lineages mediate pressure overload-induced cardiac fibrosis. *J Clin Invest*. 2014;124:2921-2934.
19. Ubil E, Duan J, Pillai IC, Rosa-Garrido M, Wu Y, Bargiacchi F, Lu Y, Stanbouly S, Huang J, Rojas M, Vondriska TM, Stefani E, Deb A. Mesenchymal-endothelial transition contributes to cardiac neovascularization. *Nature*. 2014;514:585-590.
20. Miquerol L, Thireau J, Bideaux P, Sturny R, Richard SJ, Kelly RG. Endothelial Plasticity Drives Arterial Remodeling Within the Endocardium Following Myocardial Infarction. *Circ Res*. 2015;116:1765-1771.
21. Chen Q, Zhang H, Liu Y, Adams S, Eilken H, Stehling M, Corada M, Dejana E, Zhou B, Adams RH. Endothelial cells are progenitors of cardiac pericytes and vascular smooth muscle cells. *Nat Commun*. 2016;7:12422.
22. Ali SR, Ranjbarvaziri S, Talkhabi M, Zhao P, Subat A, Hojjat A, Kamran P, Muller AM, Volz KS, Tang Z, Red-Horse K, Ardehali R. Developmental Heterogeneity of Cardiac Fibroblasts Does Not Predict Pathological Proliferation and Activation. *Circ Res*. 2014;115:625-635.
23. He L, Huang X, Kanisicak O, Li Y, Wang Y, Li Y, Pu W, Liu Q, Zhang H, Tian X, Zhao H, Liu X, Zhang S, Nie Y, Hu S, Miao X, Wang QD, Wang F, Chen T, Xu Q, Lui KO, Molkentin JD, Zhou B. Preexisting endothelial cells mediate cardiac neovascularization after injury. *J Clin Invest*. 2017;127:2968-2981.
24. Madisen L, Zwingman TA, Sunkin SM, Oh SW, Zariwala HA, Gu H, Ng LL, Palmiter RD, Hawrylycz MJ, Jones AR, Lein ES, Zeng H. A robust and high-throughput Cre reporting and characterization system for the whole mouse brain. *Nat Neurosci*. 2010;13:133-140.
25. Tian X, Pu WT, Zhou B. Cellular Origin and Developmental Program of Coronary Angiogenesis. *Circ Res*. 2015;116:515-530.
26. Liu Q, Hu T, He L, Huang X, Tian X, Zhang H, He L, Pu W, Zhang L, Sun H, Fang J, Yu Y, Duan S, Hu C, Hui L, Zhang H, Quertermous T, Xu Q, Red-Horse K, Wythe JD, Zhou B. Genetic targeting of sprouting angiogenesis using Apln-CreER. *Nat Commun*. 2015;6:6020.
27. Patel J, Seppanen EJ, Rodero MP, Wong HY, Donovan P, Neufeld Z, Fisk NM, Francois M, Khosrotehrani K. Functional Definition of Progenitors Versus Mature Endothelial Cells Reveals Key SoxF-Dependent Differentiation Process. *Circulation*. 2017;135:786-805.
28. Luxán G, D'Amato G, MacGrogan D, de la Pompa JL. Endocardial Notch Signaling in Cardiac Development and Disease. *Circ Res*. 2016;118:e1-e18.
29. Grego-Bessa J, Luna-Zurita L, del Monte G, Bolos V, Melgar P, Arandilla A, Garratt AN, Zang H, Mukouyama YS, Chen H, Shou W, Ballestar E, Esteller M, Rojas A, Perez-Pomares JM, de la Pompa JL. Notch signaling is essential for ventricular chamber development. *Dev Cell*. 2007;12:415-429.
30. Zhang H, Pu W, Liu Q, He L, Huang X, Tian X, Zhang L, Nie Y, Hu S, Lui KO, Zhou B. Endocardium Contributes to Cardiac Fat. *Circ Res*. 2016;118:254-265.
31. Fioret BA, Heimfeld JD, Paik DT, Hatzopoulos AK. Endothelial cells contribute to generation of adult ventricular myocytes during cardiac homeostasis. *Cell Rep*. 2014;8:229-241.
32. Sedmera D, Pexieder T, Vuillemin M, Thompson RP, Anderson RH. Developmental patterning of the myocardium. *Anat Rec*. 2000;258:319-337.
33. Tian X, Li Y, He L, Zhang H, Huang X, Liu Q, Pu W, Zhang L, Li Y, Zhao H, Wang Z, Zhu J, Nie Y, Hu S, Sedmera D, Zhong TP, Yu Y, Zhang L, Yan Y, Qiao Z, Wang Q-D, Wu SM, Pu WT, Anderson RH, Zhou B. Identification of a hybrid myocardial zone in the mammalian heart after birth. *Nat Commun*. 2017;8:759.

FIGURE LEGENDS

Figure 1. *Npr3-CreER* labels endocardial cells in adult heart. A, Whole mount fluorescence view of 8 weeks' adult *Npr3-CreER;R26-tdTomato* heart. Hearts were collected within 48 hours after tamoxifen treatment. **B**, Fluorescence view of whole heart section stained with tdTomato and DAPI. Boxed areas are magnified on C-E. LA, left atrium; RA, right atrium; LV, left ventricle; RV, right ventricle; VS, ventricular septum. **C-E**, Magnified images of LA, LV and RV regions from B. Arrowheads indicate $tdTomato^+PECAM^+$ endocardial cells. **F**, Immunostaining for tdTomato and aSMA on heart section shows no $tdTomato^+$ coronary arteries. **G**, Immunostaining for tdTomato and coronary endothelial cell marker FABP4 on heart sections. Arrowheads indicate $tdTomato^+FABP4^-$ endocardial cells. **H**, Quantification on the percentage of $tdTomato^+$ endocardial (Endo.) cells. Data are mean ± SEM.; n = 5. **I**, Cartoon image showing *Npr3-CreER* labels endocardial (Endo) cells but not coronary endothelial cells (CoECs). Scale bars, 1 mm in A,F; 100 μm in C-E,G.

Figure 2. Endocardial cells in the adult heart do not generate new blood vessels. A, Schematic figure showing experimental strategy. **B**, Immunostaining for tdTomato and PECAM on P20w heart section. **C**, Magnified images showing the labeling of endocardial cells in atrium, right and left ventricle. Asterisk indicated endocardial tunnel. **D**, Immunostaining for tdTomato and FABP4 on P20w heart section. **E**, Immunostaining for tdTomato and aSMA on heart section. **F**, Immunostaining for tdTomato and VE-CAD on *Npr3-CreER;R26-tdTomato* mice heart after CellTracker Green CMFDA dye injection into cardiac chamber. Asterisk indicates endocardial tunnel. **G**, Isolation of $CD31^+$ $tdTomato^+$ and $CD31^+$ tdTomato cell populations from adult *Npr3-CreER;R26-tdTomato* heart by flow cytometry. **H**, qRT-PCR of *Cd31*, *Npr3*, *Fabp4* and *Apln* expression. Data are mean ± SEM; n = 4-5; n.s., non-significant; $*P < 0.05$. **I**, Immunostaining for tdTomato and PECAM on heart section. **J**, Quantification of the percentage of tdTomato+ coronary endothelial cells in the inner myocardial wall. n = 5. Scale bars, 1 mm in B,D,E,G; 100 μm in C. Each image is representative of 5 individual samples.

Figure 3. Adult endocardial cells minimally contribute to coronary vessels after cardiac injuries. A, Immunostaining for tdTomato and FABP4 on heart sections after moderate MI injury. **B,C**, Magnified images showing that the majority of $tdTomato^+$ cells are $FABP4^-$. **D**, Quantification of the percentage of $tdTomato^+$ cells in endocardial cells (Endo.) or coronary endothelial cells (CoECs) in the border or infarct regions of the moderate MI heart. Data are mean ± SEM.; n = 5. **E**, Immunostaining for tdTomato and aSMA on MI heart section. Boxed regions are magnified in E1 and E2. **F**, Immunostaining for tdTomato and VE-CAD on MI heart section. **G-I**, Immunostaining for tdTomato and VE-CAD (G), FABP4 (H), aSMA (I) on IR heart sections. Dotted line indicates injured myocardium region. **J**, Immunostaining for tdTomato and PECAM on TAC heart section. Magnified image shows the labeling of endocardial in the left ventricle. **K**,**L**, Immunostaining for tdTomato and FABP4 (K) or aSMA (L) on TAC heart sections. **M**, Cartoon image showing that endocardial cells minimally contribute to CoECs after MI, IR or TAC injury models. Scale bars, yellow, 1 mm; white, 100 μm. Each figure is representative of 5 samples.

Figure 4. Entrapped endocardial cells contributed minimally to vascular endothelial cells in injured myocardium. A, Isolation of $CD31^+tdTomato^+$ cells from *Npr3-CreER;R26-tdTomato* mice, and subsequent transplantation into infarcted myocardium. **B**, Schematic figure showing experimental strategy. **C**, Immunostaining for tdTomato, PECAM or FABP4 on heart sections from different time points after MI. **D**, Quantification of the percentage of $FABP4^+$ vessels in transplanted $tdTomato^+$ cells (above); and also the percentage of transplanted $tdTomato^+$ cells in $FABP4^+$ vessels. Data are mean ± SEM.; n = 5. **E**, Immunostaining for tdTomato on sections of mice fused with FITC-labeled BS1 lectin (green) before sacrifice. **F**, Schematic figure showing purse-string suture-like (PSSL) model on myocardium for entrapment of endocardium through constriction of myocardium. Epi., epicardium; LV, left ventricle; VS, ventricular septum. **G**, Sirius red staining showing myocardial infarction after PSSL operation. **H**, Immunostaining for tdTomato and FABP4 on heart sections after PSSL model. Yellow arrowheads indicate

tdTomato^{+}FABP4^{+} endothelial cells. White arrowheads indicate tdTomato^{+}FABP4^{-} endocardial cells. Endo., endocardium. Asterisk indicates injured region. **I**, Immunostaining for tdTomato, VE-CAD and aSMA on tissue section shows endocardium derived cells gain part of arterial endothelial cell properties (arrowheads). **J**, Schematic figure showing trapped endocardial cells gain vascular endothelial cell property (yellow). Each image is representative of 5 individual heart samples. Scale bars, 100 μm.

NOVELTY AND SIGNIFICANCE

What Is Known?

- During fetal and neonatal stages, endocardial cells give rise to coronary blood vessels.
- In the adult heart, pre-existing coronary endothelial cells mediate neovascularization mainly after cardiac injury.
- Adult endocardial cells have been reported to be an important source of coronary vessels after myocardial infarction.

What New Information Does This Article Contribute?

- A new genetic tool *Npr3-CreER* efficiently and specifically labels endocardium in the adult heart.
- Endocardial cells in adult heart minimally contribute to coronary vessels during cardiac homeostasis or after injuries.
- Entrapped endocardium has the potential to exhibit vascular properties in the injured myocardium.

The regeneration of new coronary blood vessels after injury is of utmost clinical importance to the treatment of ischemic heart diseases. Understanding the potential of adult endocardial cells to regenerate coronary vessels has significant implications for cardiovascular regenerative medicine. Previous studies indicate that both fetal and adult endocardial cells contribute to coronary vessels. The findings of the present study show that, unlike its fetal counterpart, the adult endocardium generates minimal, if any, coronary vessels during cardiac homeostasis or after injury. Adult endocardial cells, when entrapped in the injured myocardium, exhibit vascular properties, indicating cell position and microenvironment influence endocardial cell fate. Our work provides a unique genetic tool to study the role of adult endocardium in cardiovascular diseases, and also highlights the importance of microenvironment in regulation of endocardial cell plasticity and exploration of their vascular potential after myocardial infarction.

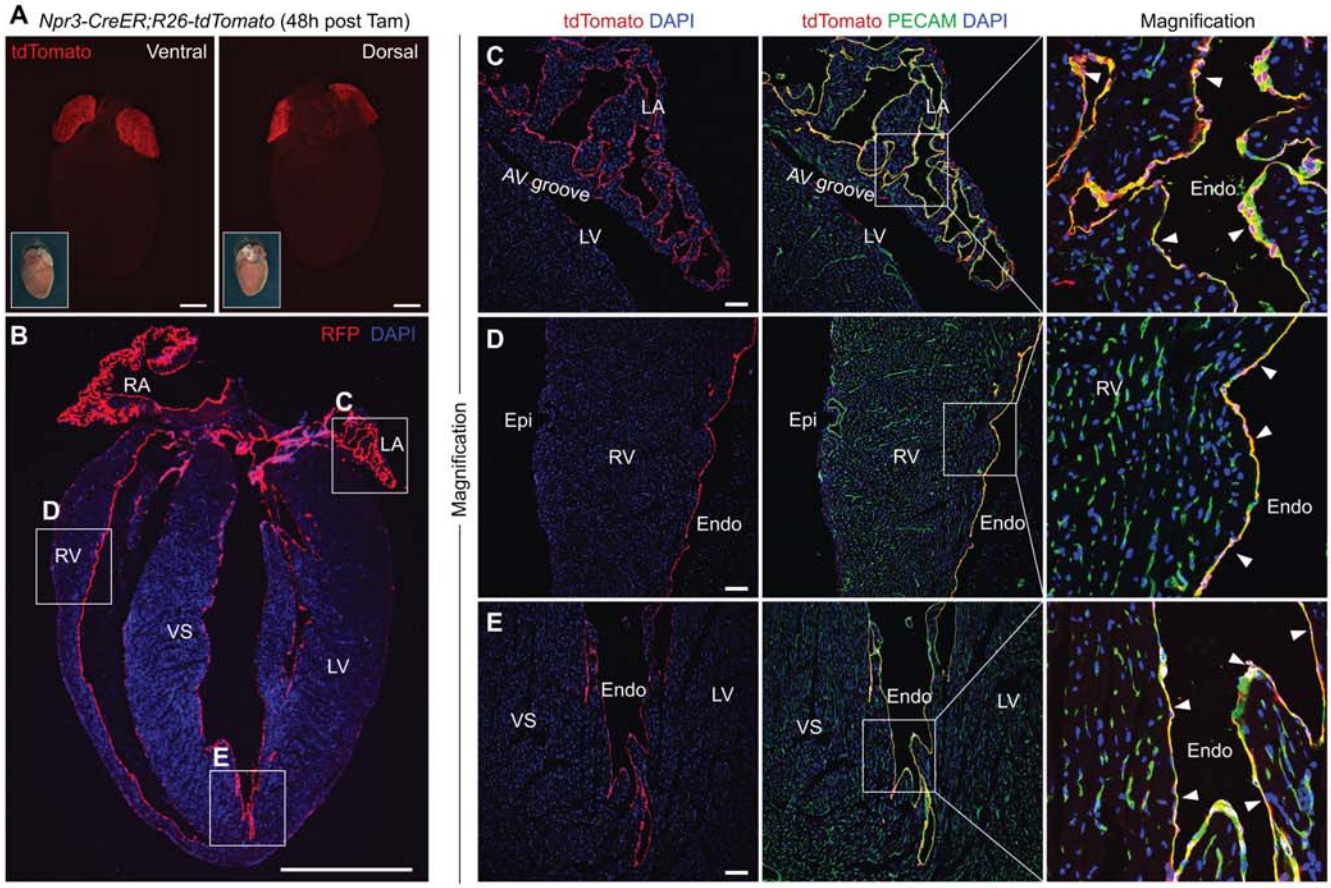

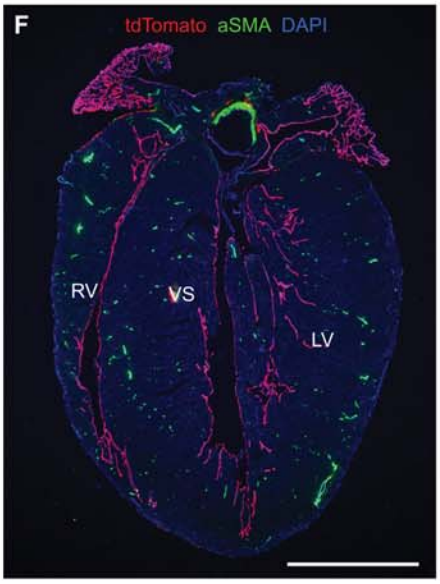

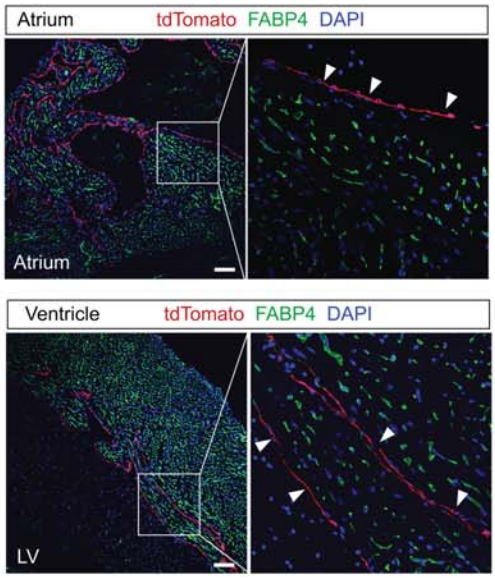

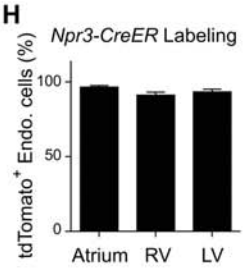

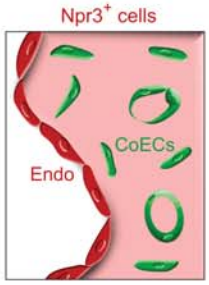

Figure 1

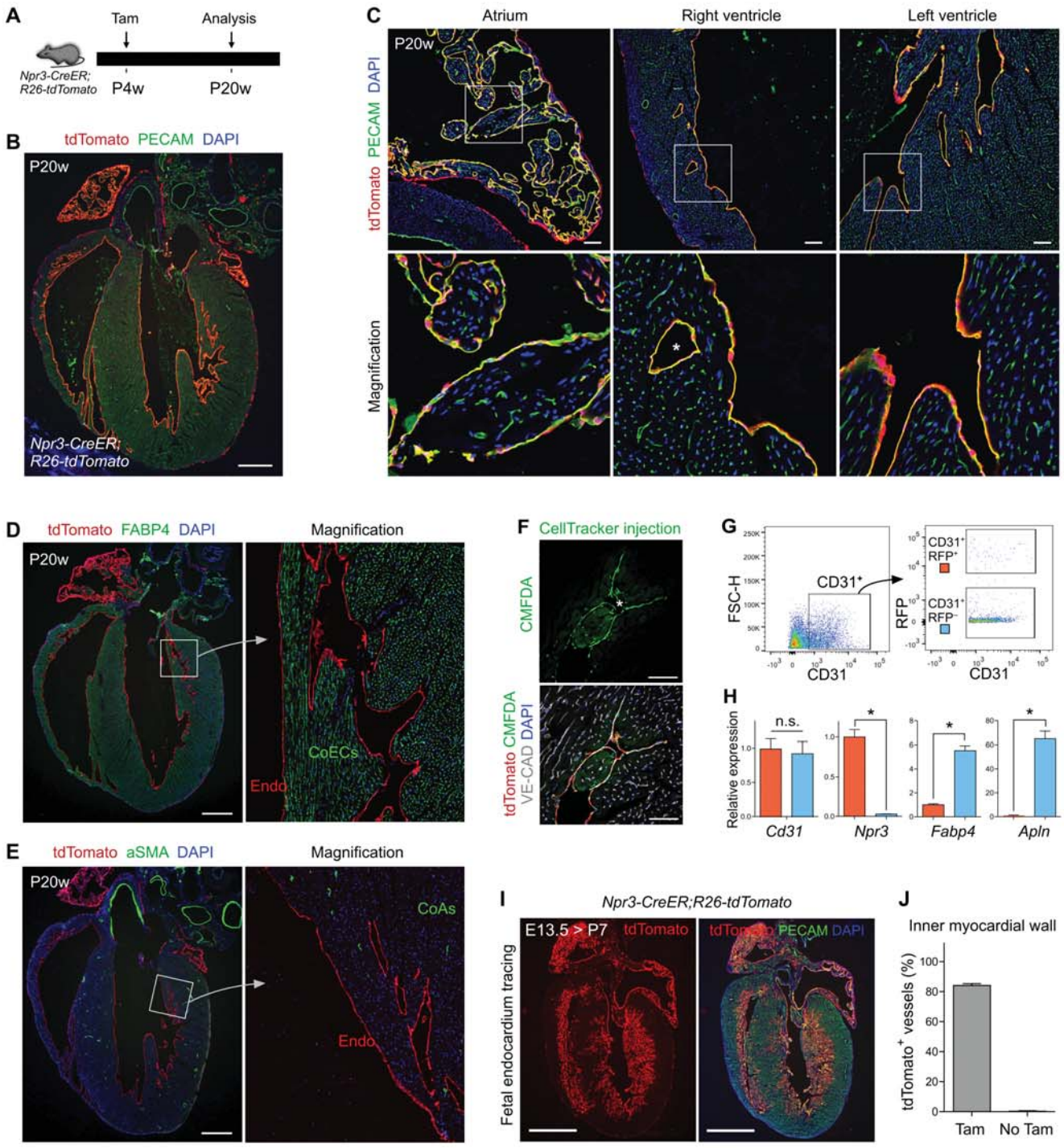

Figure 2

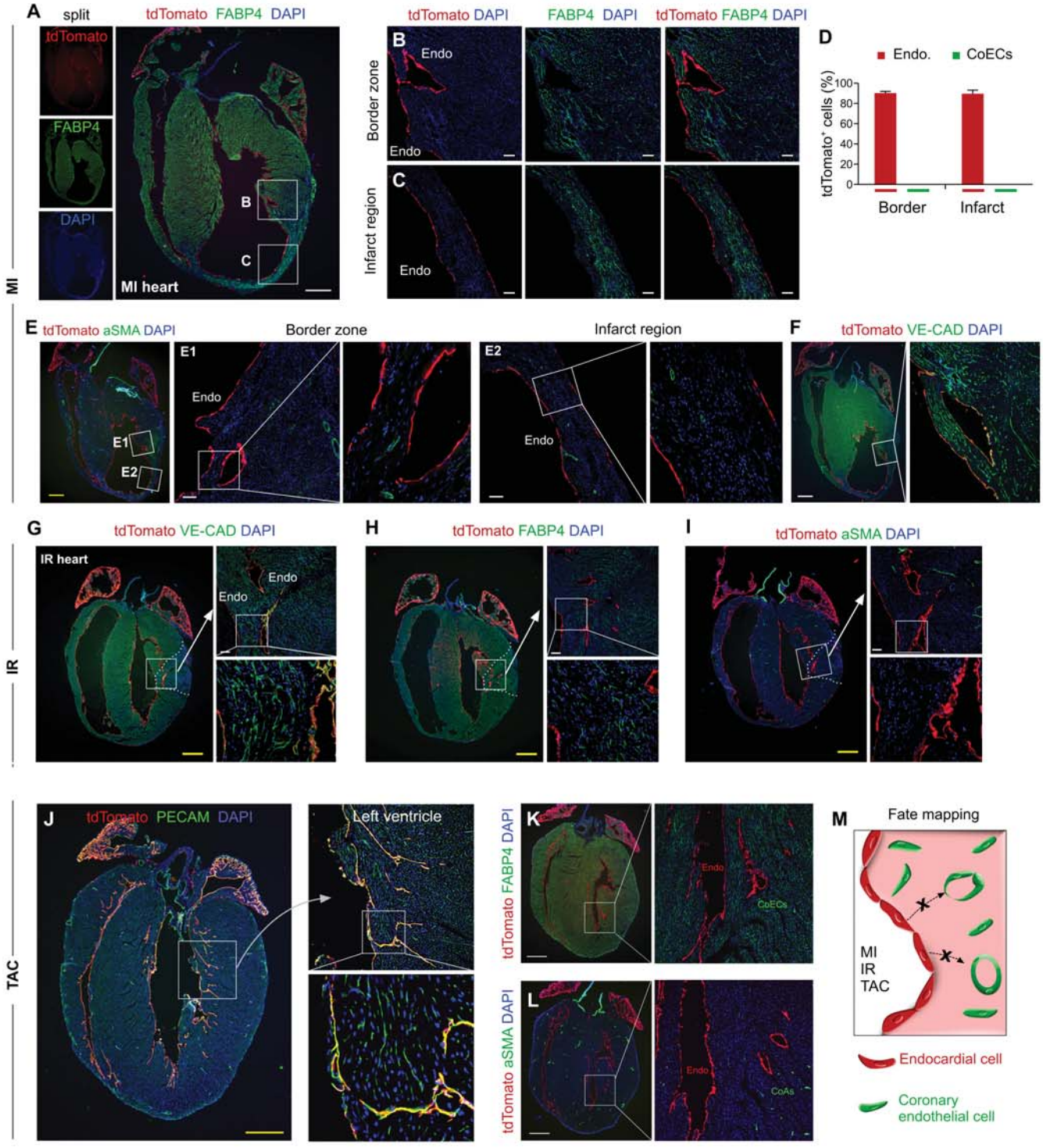

Figure 3

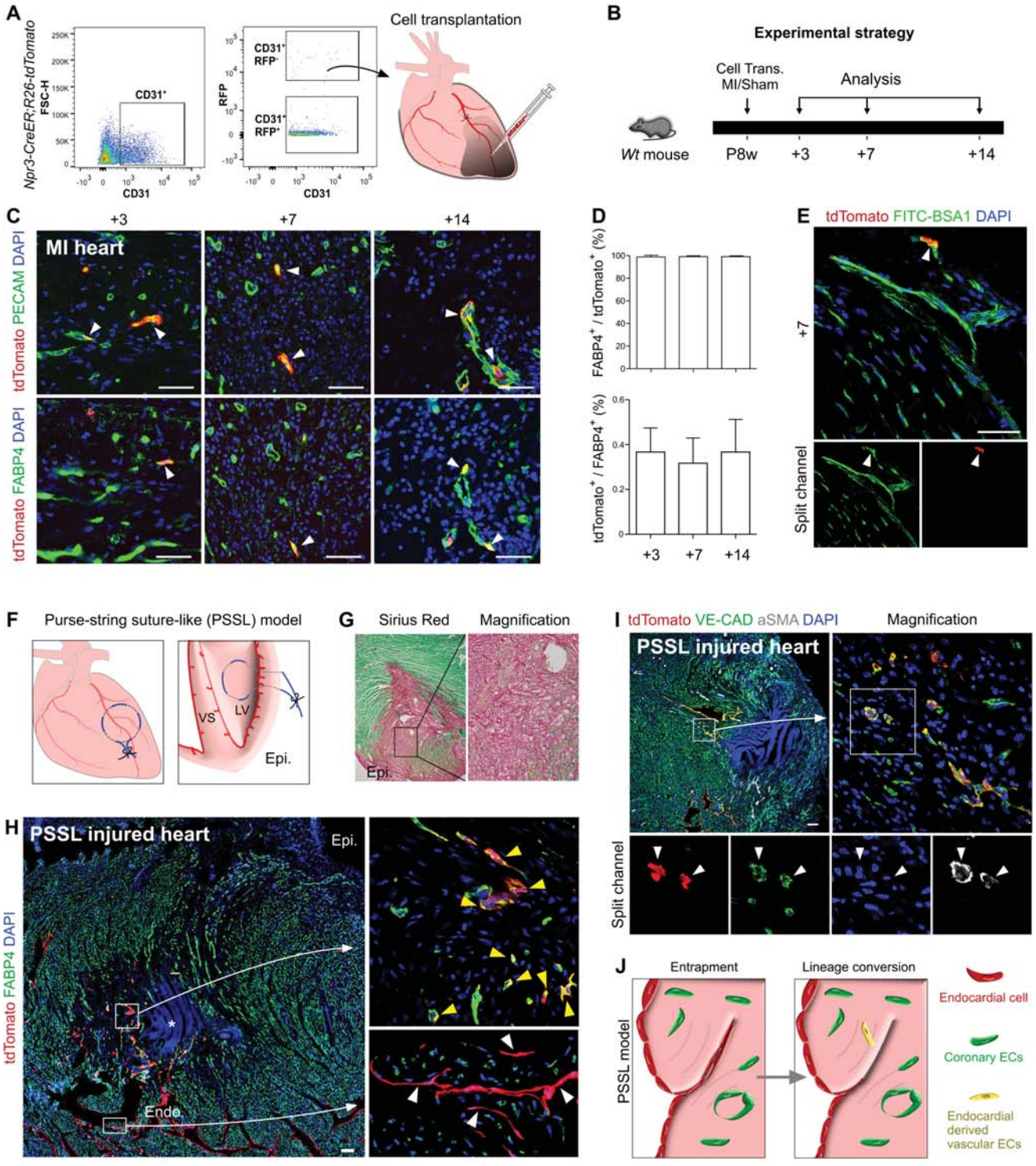

Figure 4

Genetic Fate Mapping Defines the Vascular Potential of Endocardial Cells in the Adult Heart

Juan Tang, Hui Zhang, Lingjuan He, Xiuzhen Huang, Yan Li, Wenjuan Pu, Wei Yu, Libo Zhang, Dongqing Cai, Kathy O Lui and Bin Zhou

Circ Res. published online January 26, 2018;
Circulation Research is published by the American Heart Association, 7272 Greenville Avenue, Dallas, TX 75231

Print ISSN: 0009-7330. Online ISSN: 1524-4571

Genetic fate mapping defines the vascular potential of endocardial cells in the adult heart

Supplemental Materials

A. Detailed Materials and Methods

B. Supplemental References

C. Supplemental Figures (Online Figure I -XI)

A. Detailed Materials and Methods

Mice Breeding and tamoxifen-induced lineage tracing

All mice studies were approved by the Institutional Animal Care and Use Committee (IACUC) at the Institute for Nutritional Sciences, and the institute of Biochemistry and Cell Biology, Shanghai Institutes for Biological Sciences, Chinese Academy of Science, as well as the number of animals to be used were approved based on the experiments effects size. *Npr3-CreER, Apln-CreER*, *WT1-CreER, R26R-tdTomato* mouse lines were described previously.[1–4] Briefly, *Npr3-CreER* mice was generated by conventional homologous recombination in ES cells, a cDNA encoding $CreER^{T2}$ recombinase was inserted into the translational stop codon of Npr3 gene and subsequent blastocyst injection of correctly targeted ES cell clones. All mice lines were maintained on a C57BL6/ICR background. Tamoxifen dissolved in corn oil (20 mg/ml) was introduced by gavage at the indicated time (0.1-0.2mg/g mouse body weight) for both male and female mice. For detail, *Npr3-CreER;R26R-tdTomato* mice were treated with tamoxifen at 4 weeks old and were sacrificed at young adult 20 weeks and 62 weeks aged mice for experiments. For injury model, *Npr3-CreER; R26R-tdTomato* mice were injected with tamoxifen at 8-10 weeks, one week following cessation of tamoxifen, these mice were subjected to myocardiac infarction, ischemic-reperfusion, transverse aortic constriction cardiac injury and purse-string suture like model. After indicated time, mice were sacrificed by CO_2 asphyxiation and hearts were collected for further experiments. For *Apln-CreER;R26R-tdTomato* mice

lines, we induced efficient labeling by multiple times of tamoxifen treatment from embryonic to adult stages before cardiac injury. These mice were used for EdU labeling and further study after 3 days injury. For *WT1-CreER;R26R-tdTomato* mice lines, mice were treated with tamoxifen every 2 days for 3 times. After washout for 2 weeks, myocardiac infarction and ischemic-reperfusion injury models were performed in these mice.

Mouse model of cardiac injuries

Left anterior descending (LAD) ligation was used in adult mice (8–10 weeks old) to induce myocardial infarction (MI).[5] Briefly, *Npr3-CreER;R26R-tdTomato, Apln-CreER;R26R-tdTomato* and *WT1-CreER;R26R-tdTomato* mice (both male and female) were anesthetized with isoflurane (2%) using an induction chamber and the core temperature of the animal was maintained by placement upon a 37°C water-heated pad. The breath of mice was controlled at about 120 ~ 140 breaths per minute and the respiratory volume to 0.3-0.5 mL. A vertical 1-1.5 cm incision was made between the 3rd and 4th ribs. Then the LAD coronary artery was completely ligated with a 0-8 suture permanently at the upper 1/3 location of the expose hearts. Finally, the chest and skin were closed with a 6-0 suture and the respiratory machine was kept on to ventilate mice with oxygen until *Npr3-CreER;R26R-tdTomato* mice woke up. At 21 days after LAD ligation, the mouse hearts were harvested for analysis.

Myocardial ischemia-reperfusion (IR) cardiac injury was performed in adult mice as described previously.[6] *Npr3-CreER;R26R-tdTomato* and *WT1-CreER;R26R- tdTomato* hearts were exposed as described above. Then a 0.1 cm hose was inserted in between the suture and the LAD ligated site during the left anterior descending branch of the coronary artery ligation. After 30 minutes ligation, the hose and suture was removed and the LAD coronary artery was reperfused. Then mice were supplied with oxygen for several minutes and kept warm until they behave as normal. At 14 days after injury, the mouse hearts were harvested for further studies.

Transverse aortic constriction (TAC) was performed in adult mice as described previously.[7] In short, *Npr3-CreER;R26R-tdTomato* mice (both male and female) were

anesthetized with isoflurane (2%) mixed with 0.5-1L/min 100% O2. The breath of mice was controlled at about 125 ~ 150 breaths per minute and a tidal volume of 0.1-0.3ml. After several steps of preparation and intubation of mice, forceps were used to separate the thymus and fat tissue from the aortic arch under the surgical microscope. Then a small piece of a 6.0 silk suture is placed between the innominate and left carotid arteries and two loose knots are tied around the transverse aorta, at the same time, a small piece of a 27½ gauge blunt needle is placed parallel to the transverse aorta. After two quickly tied against the needle, the needle promptly removed in order to yield a constriction of 0.4mm in diameter. Finally, the skin is closed using a 6.0 prolene suture with a continuous suture pattern. The mice were allowed to recover on heating pad until they woke up. Four weeks after TAC, hearts were collected.

Mouse heart cryoinjury (CI) were performed in 8–10 weeks old adult mice as described.[8] *Npr3-CreER;R26R-tdTomato* mice were subjected to anesthesia by freezing for 3-5 min, and then were placed on the frozen operation table once breathing was steady. The heart was exposed through a left lateral thoracotomy. Then blunt port copper wire was frozen to −70°C and used to induce frostbite by put on the heart left ventricle. The cryoinjured area was macroscopically identified as a white disk-shaped region on the left ventricle after 7 second touch with wire. After the injury, the chest was closed and the adult mice were placed under a 37°C lamp to keep warm and received oxygen until wakening. *Npr3-CreER;R26R-tdTomato* mice were then placed back with the breeding mice as soon as they woke up. Two weeks after CI injury, hearts were collected.

Purse-String Suture-like (PSSL) model was performed in adult *Npr3-CreER; R26R-tdTomato* mice hearts. In detail, both male and female *Npr3-CreER;R26R -tdTomato* were anesthetized with isoflurane (2%) using an induction chamber and the core temperature of the animal was maintained by placement upon a 37°C water-heated pad. The breath of mice was controlled at about 120 ~ 140 breaths per minute and the respiratory volume to 0.3-0.5 mL. Then a small piece of a 8.0 silk suture was cut through the myocardium to endocardium and then the silk will through the myocardium back to heart surface, once the circle is completed the two ends of the

suture material are pulled together to cause heart areas to form pouch. At last, the skin is closed using a 6.0 prolene suture with a continuous suture pattern. Then mice were supplied with oxygen for several minutes and kept warm until they behave as normal. After 14 days, mice were sacrificed and hearts were collected for further studies.

Echocardiography

The *Npr3* wild type and *Npr3-CreER* mice cardiac function was measured with high-resolution echocardiography imaging system (Vevo 2100,Visual Sonics). Mice were anaesthetized by isoflurane inhalation (1–2%) and heart rate was maintained at 400–500 b.p.m. The mitral valve leaflet was visualized and cardiac function was evaluated include left ventricle end-diastolic diameter (LVEDD), left ventricle end systolic diameter (LVESD), intraventricular septal thickness (IVST), left ventricle posterior wall thickness (LVPWT), left ventricle ejection fraction (LVEF) and left ventricle fractional shortening (LVFS) as described before.[8]

EdU pulse-chase

For EdU labeling experiments in *Apln-CreER;R26-tdTomato* mice, adult mice were injected subcutaneously with 10 μg/g EDU one day before sacrificed. Hearts were collected and prepared for cryosection and immunostaining. Sections were stained with tdTomato and endothelial cell marker, and also EdU. EdU staining was then performed based on the Life Technologies Click-iTEdU Alexa 488 Imaging Kit (Life Technologies, C10337) according to the manufacturer's instructions.[9]

Hypoxia Analysis

Heart tissue hypoxia was detected by Hypoxyprobe-1 Omni Kit (Hypoxyprobe Inc.). Wild type mice with or without MI cardiac injuries were i.p. injected with 120 mg/kg pimonidazole HCl (25 mg/ml in 0.9%NaCl). After 60 min, hearts were harvested and fixed in 4% PFA overnight and prepared for hypoxyprobe detection according to the manufacturer's protocol as described before.[5]

Immunofluorescent Staining

Immunostaining was performed as previously described.[10] Briefly, collected adult hearts from mice were wash three times in PBS, then fixed in 4% PFA for 1 hours. After three times washing in PBS, hearts with fluorescence reporters were put on agar for the whole-mount bright field and fluorescence images photographed using the Zeiss (Zeiss AXIO Zoom. V16). Then harvested hearts were incubated in 30% sucrose overnight and embedded in optimum cutting temperature (O.C.T., Sakura). Cryosections which collected at 10 μ0 thickness were used for the staining. After air dried for 1 hour at room temperature, ere blocked with blocking buffer (5% donkey serum, 0.1% Triton X-100 in PBS) for 30 minutes at room temperature and the sections were incubated with primary abtibody overnight at 4°C. In our studies, following first antibodies were used: RFP (ChromoTek, ABIN334653, 1:1000), PECAM (BD, 553370, 1:200), VE-CAD or CDH5 (R&D, AF1002, 1:100), FABP4 (Abcam, ab13979, 1:500), Hypoxyprobe Omni Kit (rabbit antisera) (Hypoxyprobe inc, 1:100), EdU (Life Technologies, C10337, CLICK-ITEDUKit), WGA-Alexa488 (Invitrogen, W11261; 1:100), smooth muscle actin-FITC (Sigma, F3777; 1:100). Finally, Alexa fluorescence-conjugated secondary antibodies (Invitrogen) were used to detect hearts signals. While for weak signals, HRP or biotin-conjugated secondary antibodies and a tyramide signal amplification kit (PerkinElmer) were used. Images were captured under Olympus (FV1200) or Zeiss (LSM 710) laser-scanning confocal microscope from each heart.

Cell Isolation and Fluorescence activated cell sorting

Cells were isolated from adult *Npr3-CreER;R26R-tdTomato* mice as described previously.[11] Briefly, adult mice were injected with 200μl heparin (6.25 U/μl) intraperitoneally, following injection of pentobarbital sodium. Then mice hearts were dissected, carefully cut into small pieces with fine scissors and digested by several trypsinization steps at 37°C. After digestion, lysis buffer contain cells were passed through 70-mm cell strainers, washed and non-cardiomyocytes were obtained by centrifuge at 500 g for 3 min at 4 °C. Cells collected from mice hearts were stained

with fluorochrome-conjugated antibodies, according to the manufacturer's instruction. Isolated cells were first incubated with LIVE/DEAD Fixable Violet Dead Cell Stain Kit (Life Technology, L34955, 1:1000), and subsequently stained with CD31-APC (17-0311, eBioscience, 1:200) for 30 min. Fluorescence labeled cells sort was performed using a BD FACS Aria flow cytometry system (BD Biosciences, San Jose, CA), and data were analysed with FlowJo software (Tree Star, Ashland, Ore). $CD31^{+}RFP^{+}$ and $CD31^{+}RFP^{-}$ cells were collected for the further experiments.

CellTracker Green CMFDA dye tracing of ventricular endocardial cells

Npr3-CreER;R26R-tdTomato mice were induced with tamoxifen (0.1-0.2mg/g mouse body weight) at 4 weeks and hearts were harvested at 20 weeks. Atria and sinuses of collected hearts were removed and microinjected with the CellTracker Green CMFDA dye (Invitrogen) through their ventricles as reported.[12] After short time (about 1 minute) perfuse, hearts were washed with PBS for three times and prepared for cryosection and immunostaining procedures.

Quantitative RT-PCR (*qRT-PCT*) analysis

After $CD31^{+}RFP^{+}$ and $CD31^{+}RFP^{-}$ cells were isolated by flow cytometry, RNA was extracted form these two groups cells with Trizol according to the manufacturer's instruction (Invitrogen) and we the RNA were converted to cDNA by using Prime Script RT kit (Takara). SYBR Green qPCR master mix (Applied Biosystems) was used and cDNA was amplified on a StepOnePlusTM real-time PCR system (Applied Biosystems). Quantitative PCR Primers used were listed as following: Gapdh (Forward, 5'-GAAGGGCTCATGACCACAG-3', reverse, 5'-GATGCAGGGATG ATGTTCT G-3'), Pecam (Forward, 5'- TAAGGGTGGAACACTCTCTGGT-3', reverse, 5'- TGTTCTTCTCTCCCTTCAGAGG-3'), Fabp4 (Forward, 5'-CACCA TCCGGTCA GAGAGTA-3', reverse, 5'- TGATGCTCTTCACCTTCCTG-3'), Apln (Forward, 5'- GTTGCAGCATGAATCTGAGG-3', reverse, 5'-TCAGTGGCACT CCACAAAC T-3'), Npr3 (Forward, 5'-TTCTTCCTACGGAGATGGCT-3', reverse,

5’- ACGGTCCTCAGTAGGGTGAC-3’). All mRNA expression levels were normalized by comparing them to the housekeeping gene GAPDH.

Sirius Red Staining

Adult *Npr3-CreER;R26R-tdTomato* mice heart sections were collected after hearts injuried models, then Sirius red staing was applied to detect collagen desposition following protocol as described before.[6] Briefly, the sections were washed by PBS to remove OCT. After that, slides were fixed with Bouins’ solution (5% acetic acid, 9% formaldehyde and 0.9% picric acid) 55°C for 1 hour or at room temperature overnight. Next day after washing with running tape water until yellow diasappears, 0.1% Fast Green (Fisher, F-99) was used to staing slides for 3 minutes, then in 1% acetic acid for 2 minutes and in 0.1% Sirius red for 1-2 minutes. After washed 3 times with ddH2O, slides were dehydrated with ethanol and xylene based on standard procedures. Finally, we cover the slides in hood and images were acquired on Olympus BX53 microscope.

Statistical analysis

All data were determined from four independent samples and presented as mean values ± standard error of the mean (SEM). Statistical comparisons between data sets were made with analysis of normality and variance, followed by a two-sided unpaired Student's *t*-test for comparing differences between two groups, and ANOVA test for over two groups. Significance was accepted when $P < 0.05$. All mice were randomly assigned to different experimental groups. Sample sizes were designed with adequate power according to the literature and our previous studies. Randomization and blinding strategy was used whenever possible.

B. Supplemental References

1. Zhang H, Pu W, Li G, Huang X, He L, Tian X, Liu Q, Zhang L, Wu SM, Sucov HM, Zhou B. Endocardium Minimally Contributes to Coronary Endothelium in the Embryonic Ventricular Free Walls. *Circ Res*. 2016;118:1880-1893.
2. Tian X, Hu T, Zhang H, He L, Huang X, Liu Q, Yu W, He L, Yang Z, Zhang Z,

Zhong TP, Yang X, Yang Z, Yan Y, Baldini A, Sun Y, Lu J, Schwartz RJ, Evans SM, Gittenberger-de Groot AC, Red-Horse K, Zhou B. Subepicardial endothelial cells invade the embryonic ventricle wall to form coronary arteries. *Cell Res*. 2013;23:1075-1090.

3. Zhou B, Ma Q, Rajagopal S, Wu SM, Domian I, Rivera-Feliciano J, Jiang D, von Gise A, Ikeda S, Chien KR, Pu WT. Epicardial progenitors contribute to the cardiomyocyte lineage in the developing heart. *Nature*. 2008;454:109-113.
4. Madisen L, Zwingman TA, Sunkin SM, Oh SW, Zariwala HA, Gu H, Ng LL, Palmiter RD, Hawrylycz MJ, Jones AR, Lein ES, Zeng H. A robust and high-throughput Cre reporting and characterization system for the whole mouse brain. *Nat Neurosci*. 2010;13:133-140.
5. Liu Q, Hu T, He L, Huang X, Tian X, Zhang H, He L, Pu W, Zhang L, Sun H, Fang J, Yu Y, Duan S, Hu C, Hui L, Zhang H, Quertermous T, Xu Q, Red-Horse K, Wythe JD, Zhou B. Genetic targeting of sprouting angiogenesis using Apln-CreER. *Nat Commun*. 2015;6:6020.
6. He L, Huang X, Kanisicak O, Li Y, Wang Y, Li Y, Pu W, Liu Q, Zhang H, Tian X, Zhao H, Liu X, Zhang S, Nie Y, Hu S, Miao X, Wang QD, Wang F, Chen T, Xu Q, Lui KO, Molkentin JD, Zhou B. Preexisting endothelial cells mediate cardiac neovascularization after injury. *J Clin Invest*. 2017;127:2968-2981.
7. Bisping E, Ikeda S, Kong SW, Tarnavski O, Bodyak N, McMullen JR, Rajagopal S, Son JK, Ma Q, Springer Z, Kang PM, Izumo S, Pu WT. Gata4 is required for maintenance of postnatal cardiac function and protection from pressure overload-induced heart failure. *Proc Natl Acad Sci U S A*. 2006;103:14471-14476.
8. Yu W, Huang X, Tian X, Zhang H, He L, Wang Y, Nie Y, Hu S, Lin Z, Zhou B, Pu W, Lui KO, Zhou B. GATA4 regulates Fgf16 to promote heart repair after injury. *Development*. 2016;143:936-949.
9. Pu W, Zhang H, Huang X, Tian X, He L, Wang Y, Zhang L, Liu Q, Li Y, Li Y, Zhao H, Liu K, Lu J, Zhou Y, Huang P, Nie Y, Yan Y, Hui L, Lui KO, Zhou B. Mfsd2a+ hepatocytes repopulate the liver during injury and regeneration. *Nat Commun*. 2016;7:13369.
10. Zhang H, Pu W, Tian X, Huang X, He L, Liu Q, Li Y, Zhang L, He L, Liu K, Gillich A, Zhou B. Genetic lineage tracing identifies endocardial origin of liver vasculature. *Nat Genet*. 2016;48:537-543.
11. Zhang H, Huang X, Liu K, Tang J, He L, Pu W, Liu Q, Li Y, Tian X, Wang Y, Zhang L, Yu Y, Wang H, Hu R, Wang F, Chen T, Wang QD, Qiao Z, Zhang L, Lui KO, Zhou B. Fibroblasts in an endocardial fibroelastosis disease model mainly originate from mesenchymal derivatives of epicardium. *Cell Res*. 2017
12. Wu B, Zhang Z, Lui W, Chen X, Wang Y, Chamberlain AA, Moreno-Rodriguez R, Markwald R, O?Rourke B, Sharp D, Zheng D, Lenz J, Baldwin H, Chang C-P, Zhou B. Endocardial Cells Form the Coronary Arteries by Angiogenesis through Myocardial-Endocardial VEGF Signaling. *Cell*. 2012;151:1083-1096.

C. Supplemental Figures (Online Figure I -XI)

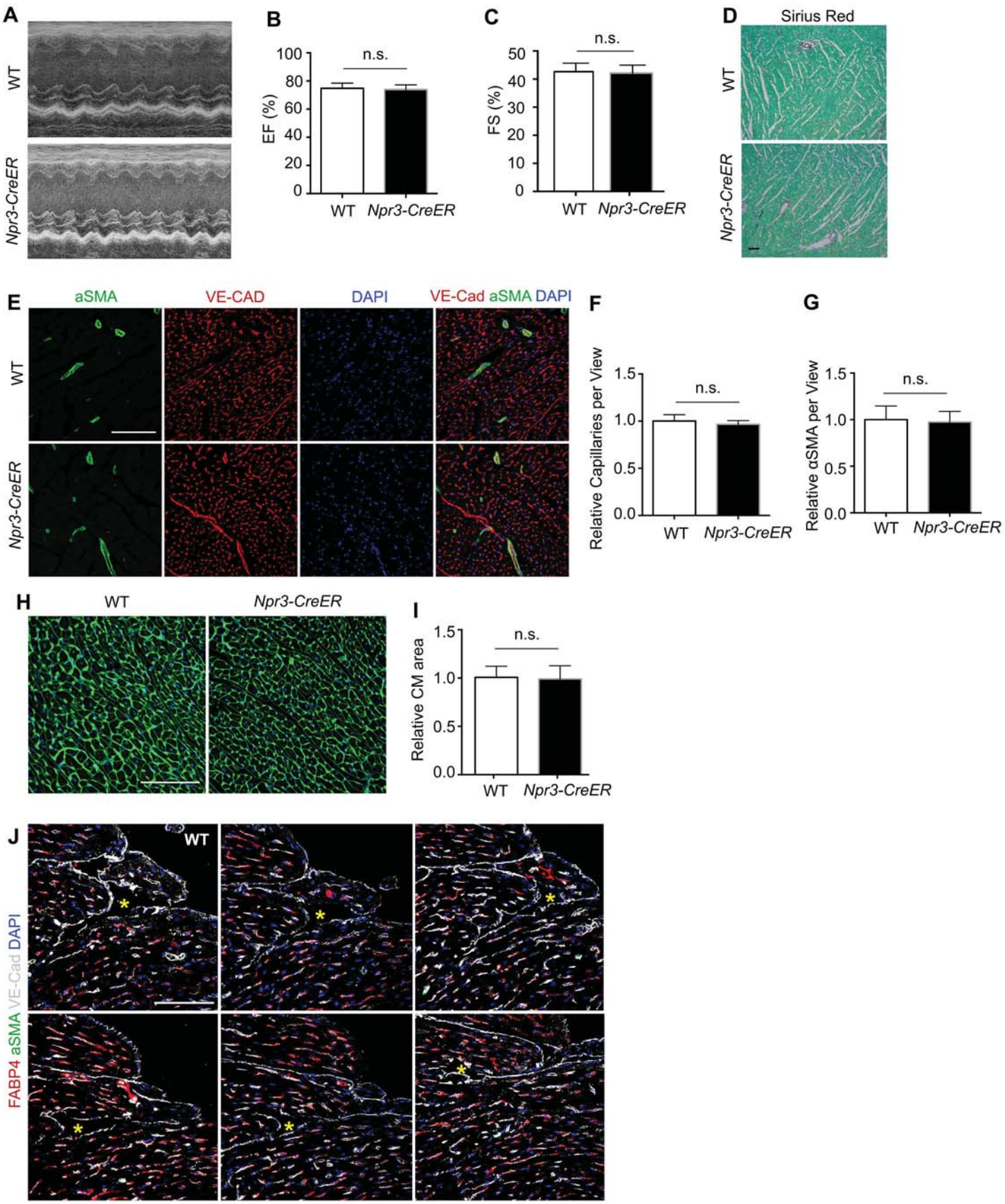

Online Figure I. Adult *Npr3-CreER* mouse does not exhibit heart defect. A, Representative echocardiography images of wild-type (WT) and *Npr3-CreER* heterozygous mice. **B**,**C**, Cardiac function of wild-type and *Npr3-CreER* mice. EF, ejection fraction. FS, fraction shorten. Data are mean ± s.e.m.; n.s., non-significant; n = 5. **D**, Representative sirius red staining of wild-type and *Npr3-CreER* heterozygous mice. **E**, Immunostaining of VE-CAD and aSMA in wild-type and *Npr3-CreER* mice heart sections. **F**,**G**, Quantitation of capillaries density (F) and aSMA cells (G) in E. Data are mean ± s.e.m.; n.s., non-significant; n = 5. **H**, Immunostaining of WGA in wild-type and *Npr3-CreER* mice heart. **I**, Quantitation of cardiomyocytes cell size in H. Data are mean ± s.e.m.; n.s., non-significant; n = 5. **J**, Immunostaining for FABP4, aSMA and VE-Cad on wild-type mice heart serial section. Asterisks indicate endocardial tunnels that are connected with cardiac chamber. n = 5. Each image is representative of 5 individual samples. Scale bars, 100 μm in D, E, H and J.

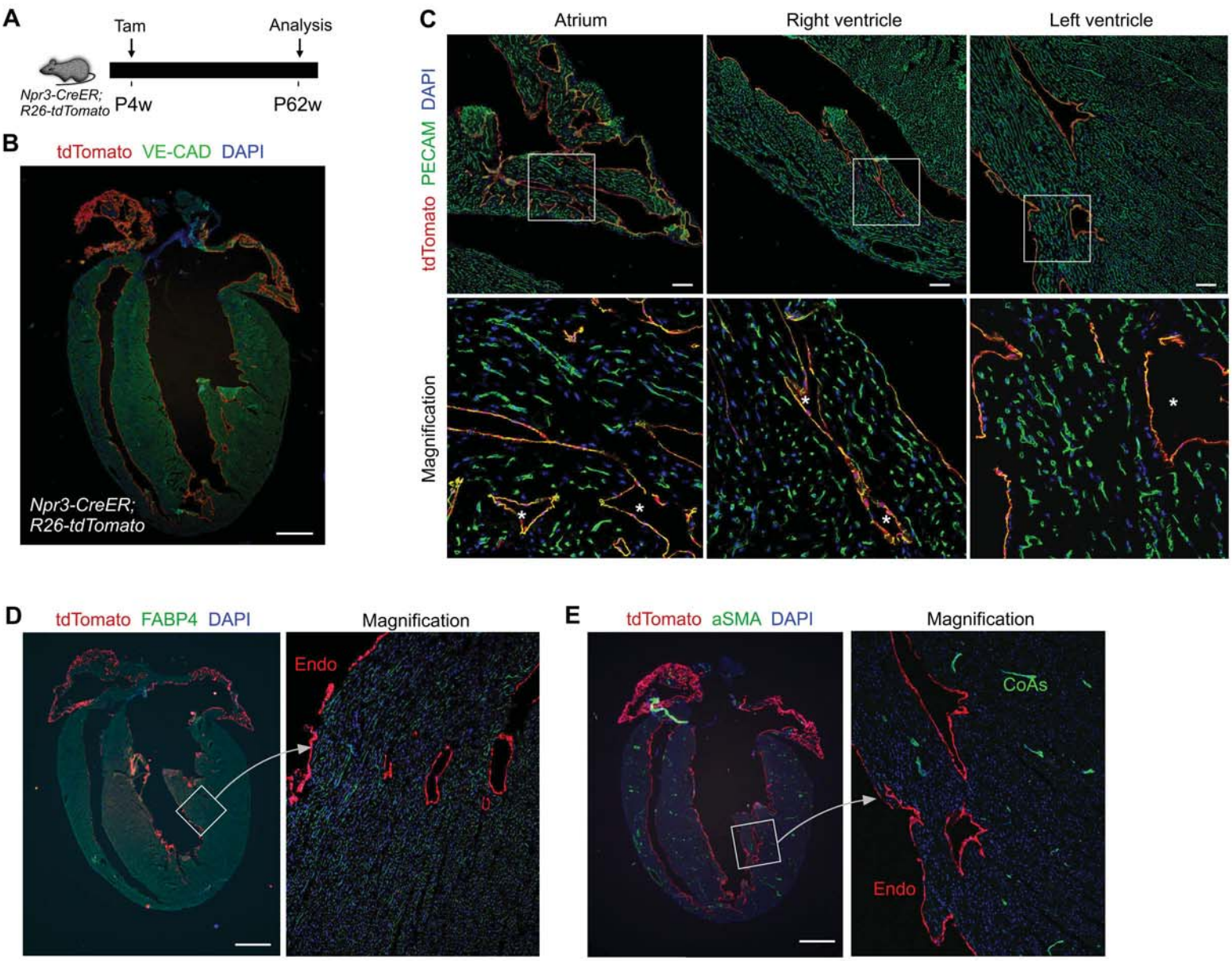

Online Figure II. Endocardial cells in the adult heart do not generate new blood vessels in 62 weeks mice. A, Schematic figure showing experimental strategy. **B**, Immunostaining for tdTomato and PECAM on heart section. **C**, Magnified images showing the labeling of endocardial cells in atrium, right and left ventricle. Asterisk indicated endocardial tunnels. **D**, Immunostaining for tdTomato and FABP4 on heart section. **E**, Immunostaining for tdTomato and aSMA on heart section. Scale bars, 1 mm in B,D,E; 100 μm in C. Each image is representative of 5 individual samples.

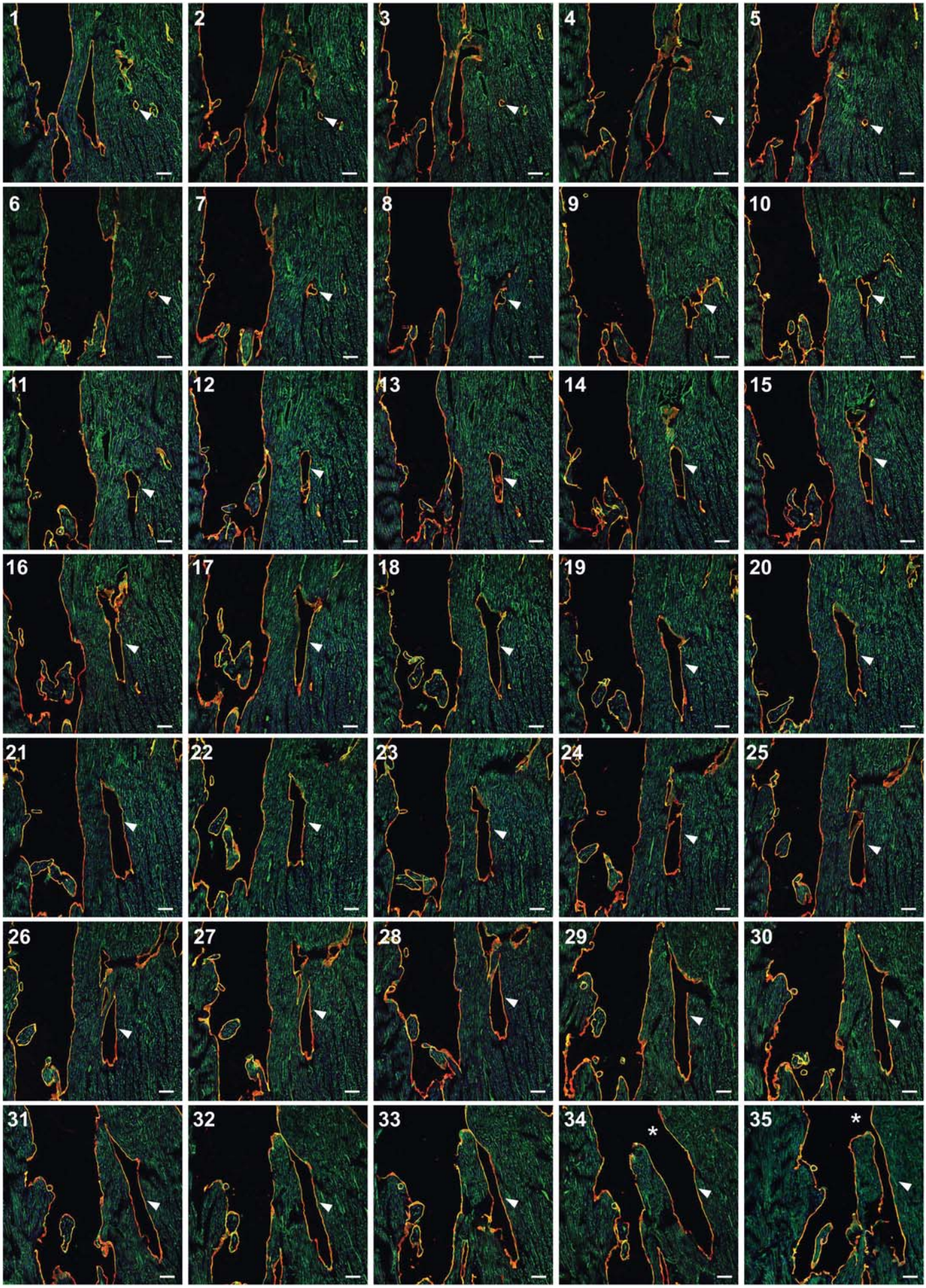

Online Figure III. Intramyocardial tdTomato^{+} tube-like structures are trapped endocardium. Immunostaining for tdTomato and PECAM on serial heart sections (1-35). Arrowheads indicate tube-like structures that are within intramyocardium in sections 1-33 and are connected with chamber circulation (asterisks) in sections 34-35. Scale bars, 100 μm.

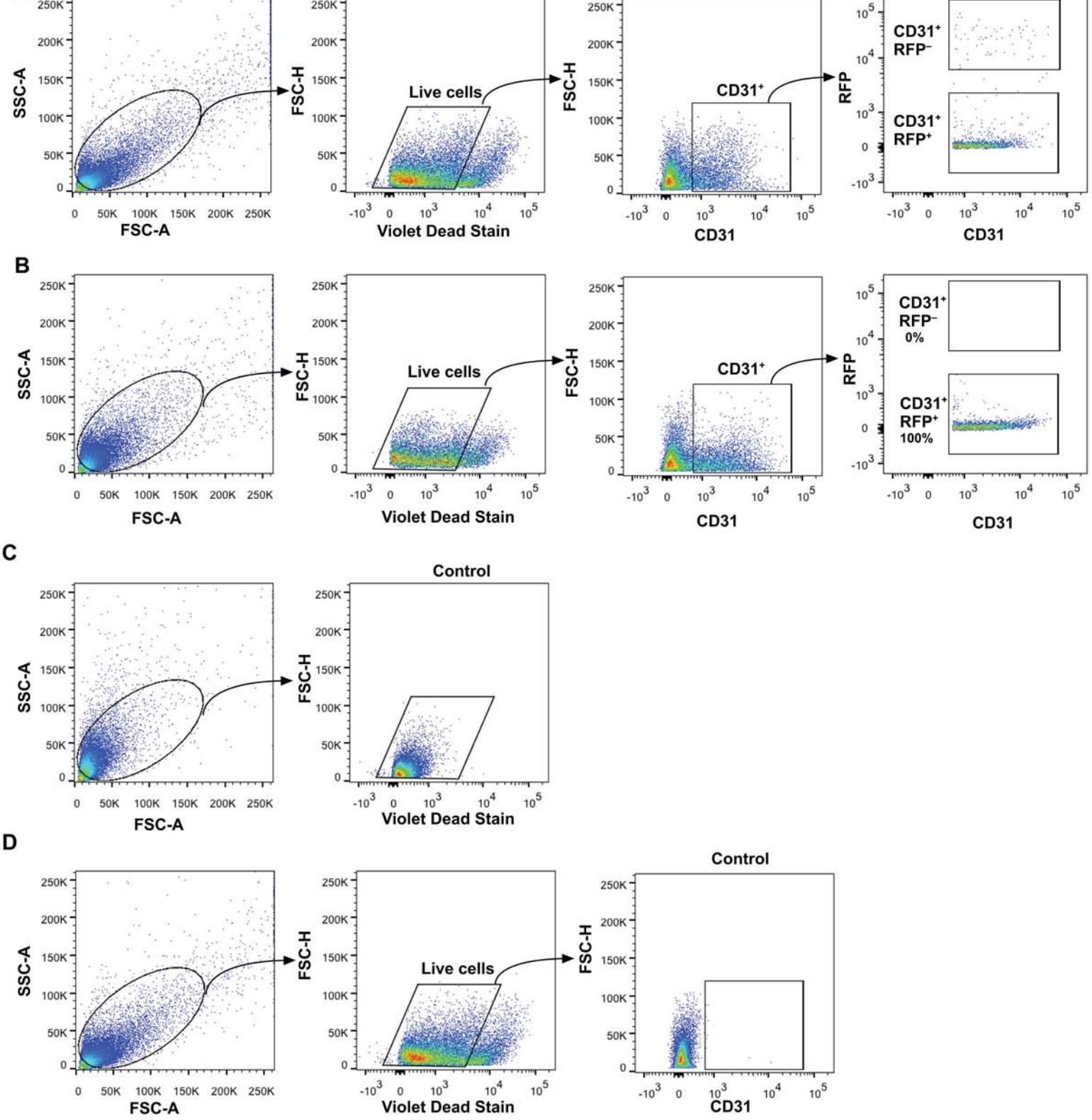

Online Figure IV. Gating strategy for CD31⁺RFP⁺ and CD31⁺RFP⁻ cell isolation. A,**B**, Flow cytometry plot gated on live CD31⁺RFP⁺ and CD31⁺RFP⁻ sequentially from *Npr3-CreER;R26-tdTomato* with tamoxifen (A) or no tamoxifen (B). **C**,**D**, Negative control for Violet dead stain (C) and CD31 (D).

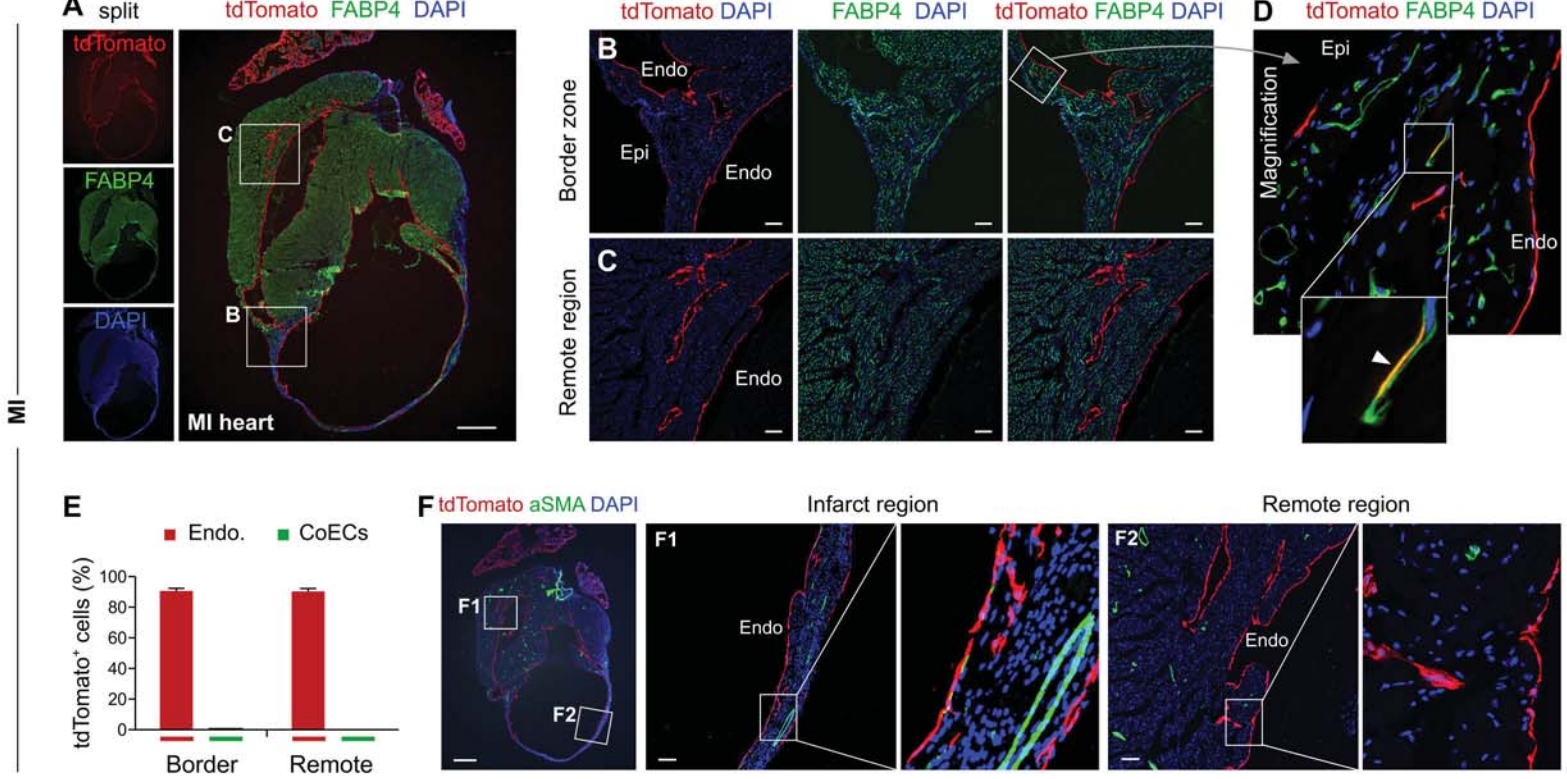

Online Figure V. Adult endocardial cells minimally contribute to coronary vessels after severe MI. A, Immunostaining for tdTomato and FABP4 on severe MI heart. **B-D**, Magnified images showing that the majority of tdTomato$^+$ cells are FABP4$^-$, and sparse tdTomato$^+$FABP4$^+$ cell (arrowhead) is detected in the border zone of MI heart (D). **E**, Quantification of the percentage of tdTomato$^+$ cells in endocardial cells (Endo.) or coronary endothelial cells (CoECs) in the border or remote regions of the MI heart. Data are mean ± s.e.m.; n = 5. **F**, Immunostaining for tdTomato and aSMA on MI heart section. Boxed regions are magnified in F1 and F2. Scale bars, 1 mm in A,F; 100 μm in others. Each figure is representative of 5 samples.

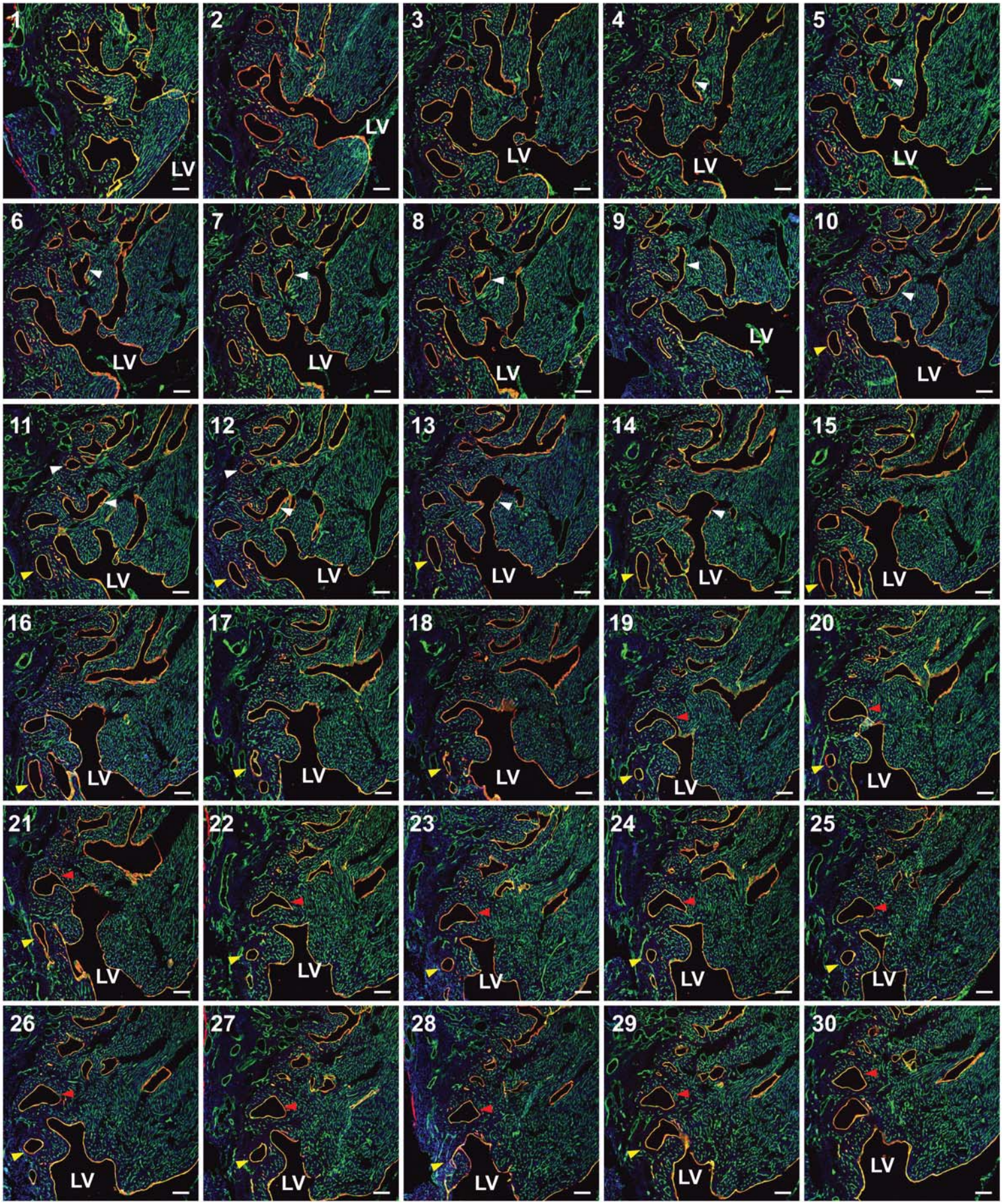

Online Figure VI. Intramyocardial tdTomato$^+$ tube-like structures are endocardial cells in MI heart. Immunostaining for tdTomato and PECAM on serial heart sections (1-30). Arrowheads in white, yellow and red colors indicate three examples of intramyocardial tube-like structures that are actually connected with left ventricular (LV) chamber. Scale bars, 100 μm.

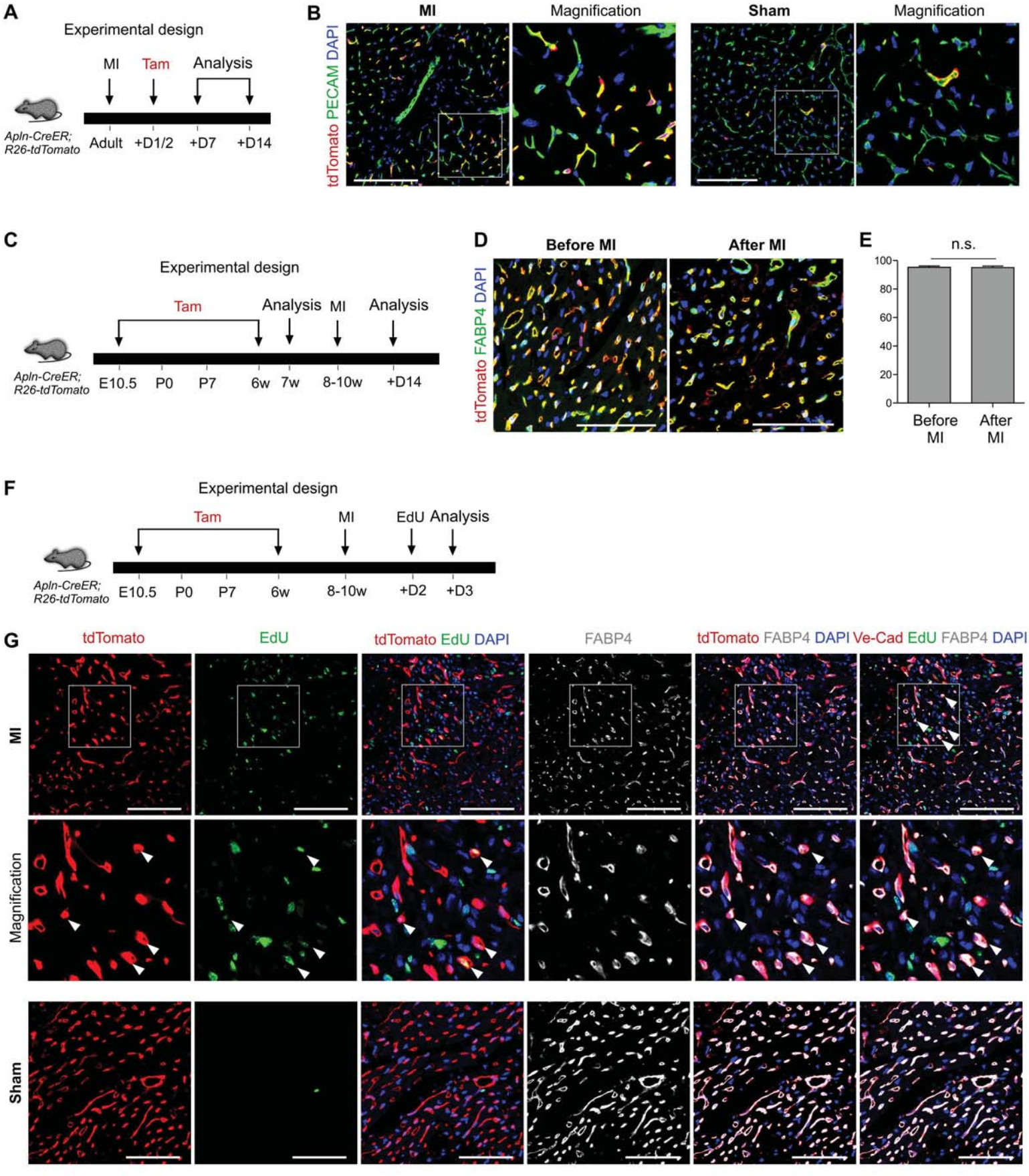

Online Figure VII. Pre-existing endothelial cells contribute to newly formed vessels in MI heart. A, Schematic figure showing experimental design. Tamoxifen (Tam) was inducted after MI to detect Apln activity in injured heart. **B**, Immunostaining for tdTomato and PECAM on heart sections shows Apln is activated after MI, compared with sham control. **C**, Schematic figure showing experimental design. Tam was induced before MI to label pre-existing vessels in the heart. **D**, Immunostaining for tdTomato and FABP4 on hearts collected before or after MI. **E**, Quantification of the percentage of vessels labeled with tdTomato. Data are mean ± SEM; n = 5; n.s., non-significant. **F**, Schematic figure showing experimental design. Tamoxifen was induced before MI and EDU was administered one day before analysis. **G**, Immunostaining for EDU, tdTomato and FABP4 on heart section. Arrowheads indicate EdU$^+$tdTomato$^+$FABP4$^+$ proliferating vascular endothelial cells that are derived from pre-existing vessels labeled by *Apln-CreER* before injury. There is rare proliferating endothelial cells detected in Sham heart samples (lower panel). Scale bars,100 μm. Each image is representative of 5 individual samples.

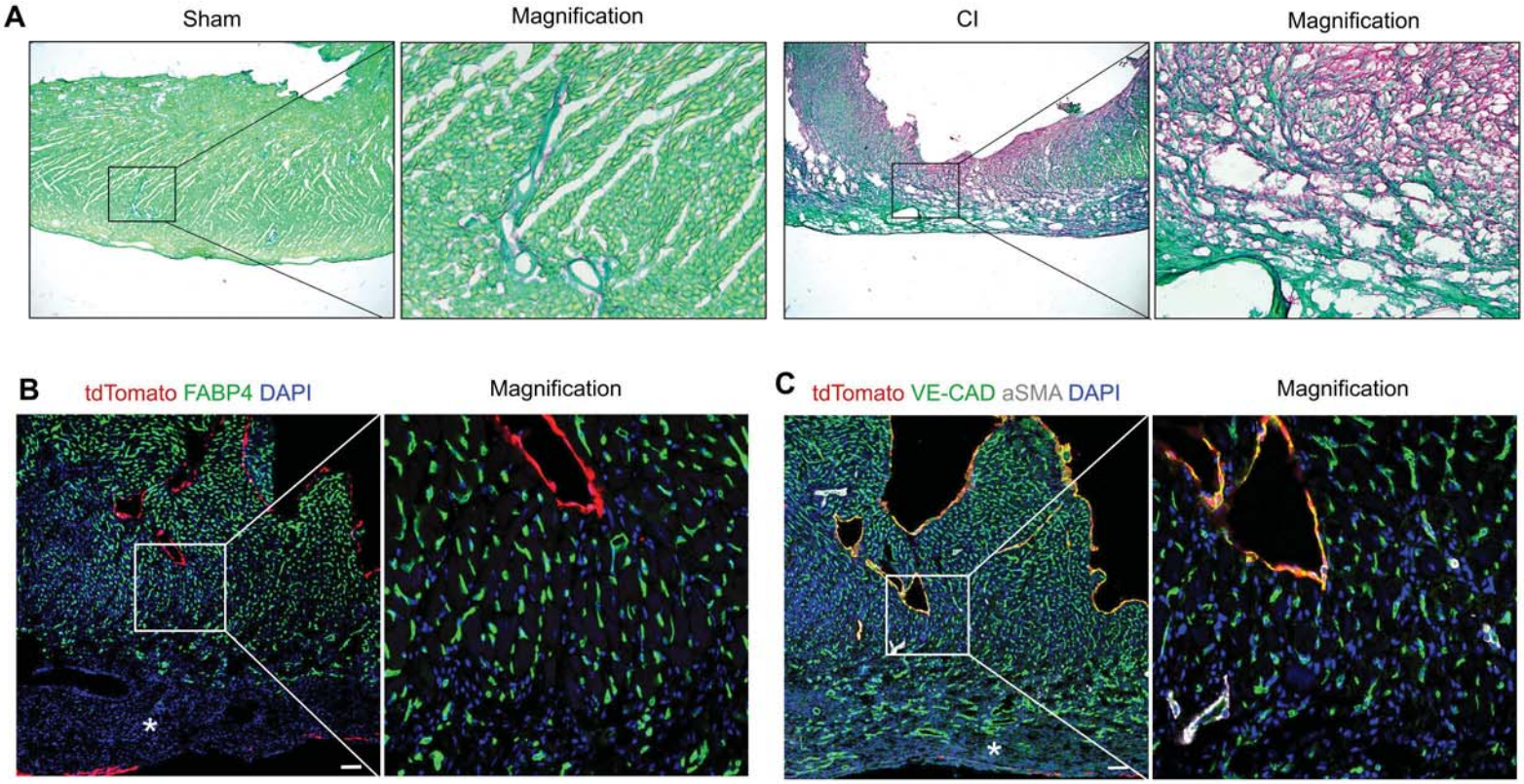

Online Figure VIII. Endocardial cells do not contribute to coronary vessels after cryo-injury (CI). A, Sirius Red staining on sham and CI heart sections. **B**, Immunostaining for tdTomato and FABP4 on CI heart. **C**, Immunostaining for tdTomato, VE-CAD and aSMA on CI heart. Asterisks indicate injured myocardium. Scale bars, 100 μm. Each figure is representative of 5 heart samples.

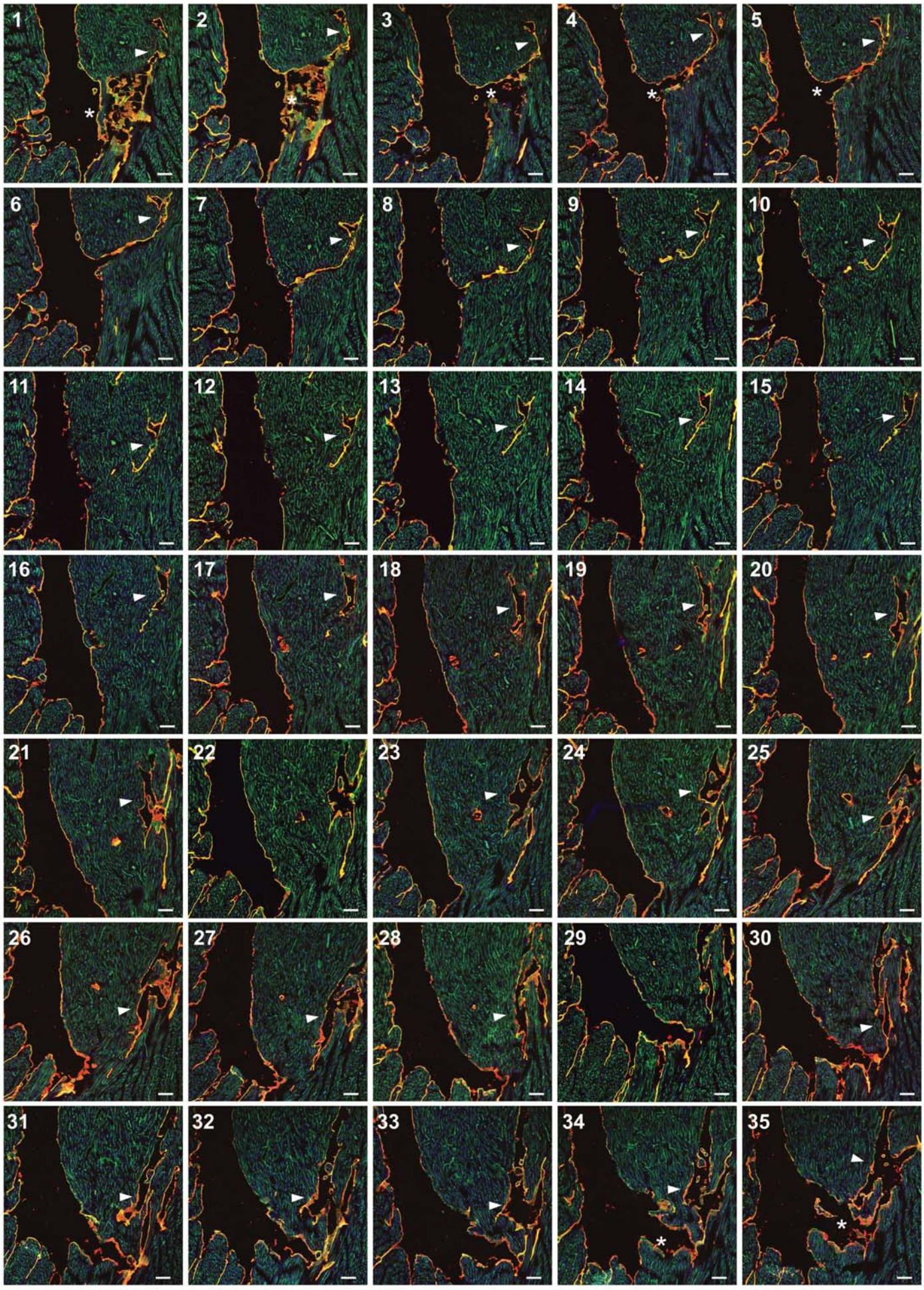

Online Figure IX. Intramyocardial tdTomato$^+$ tube-like structures are endocardial cells in TAC model. Immunostaining for tdTomato and PECAM on serial heart sections (1-35). Arrowheads indicate tube-like structures that are within intramyocardium in sections 6-33 and are connected with chamber circulation (asterisks) in sections 1-5 and sections 34-35. Scale bars, 100 μm.

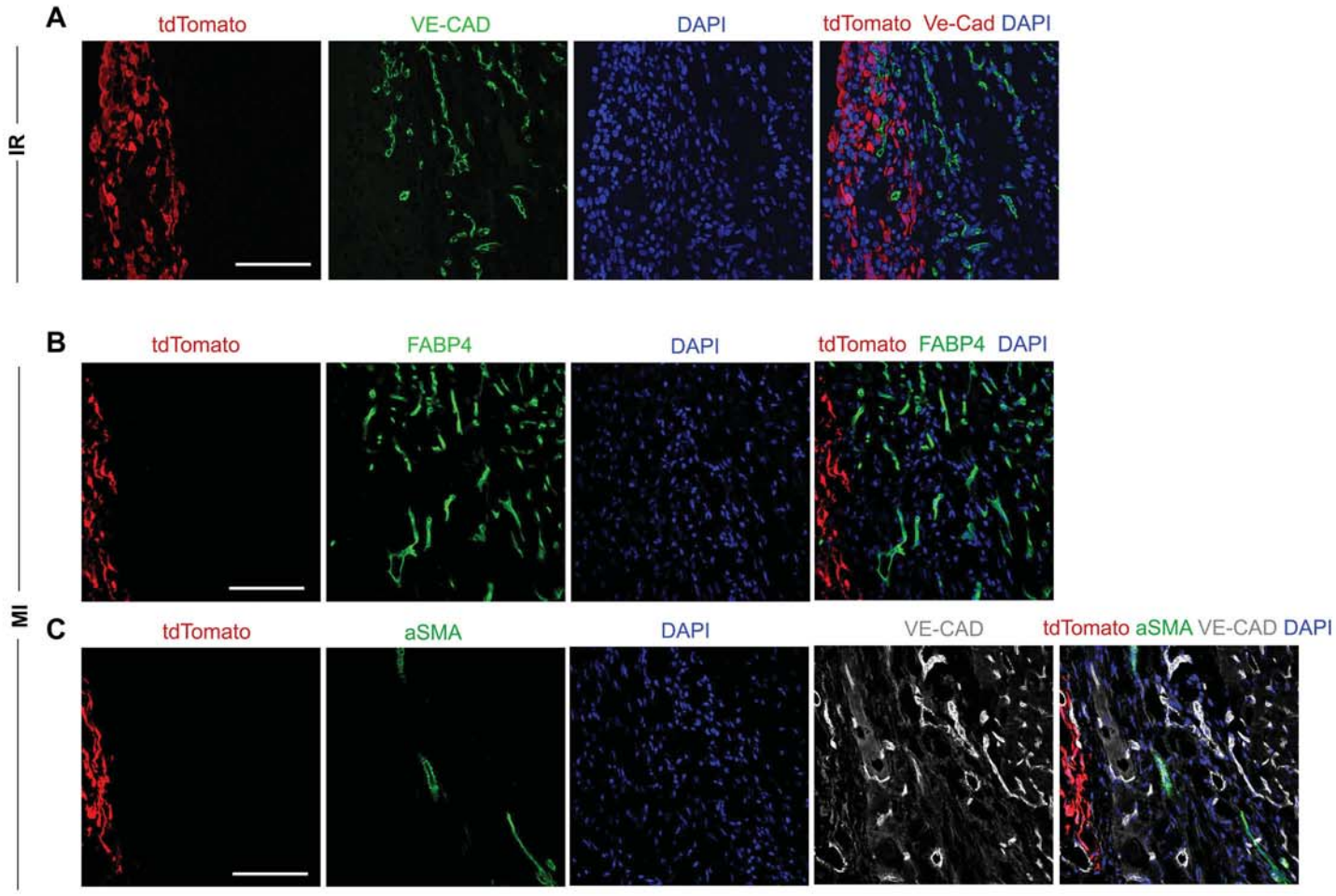

Online Figure X. Epicardium cells in the adult heart do not generate new blood vessels after cardiac injuries. A, Immunostaining for tdTomato and VE-CAD on *WT1-CreER;R26-tdTomato* heart sections after IR. **B**, Immunostaining for tdTomato and FABP4 on *WT1-CreER;R26-tdTomato* heart section after MI. **C**, Immunostaining for tdTomato, VE-CAD and aSMA on *WT1-CreER;;R26-tdTomato* heart section after MI. Scale bars, 100 μm. Each figure is representative of 5 heart samples.

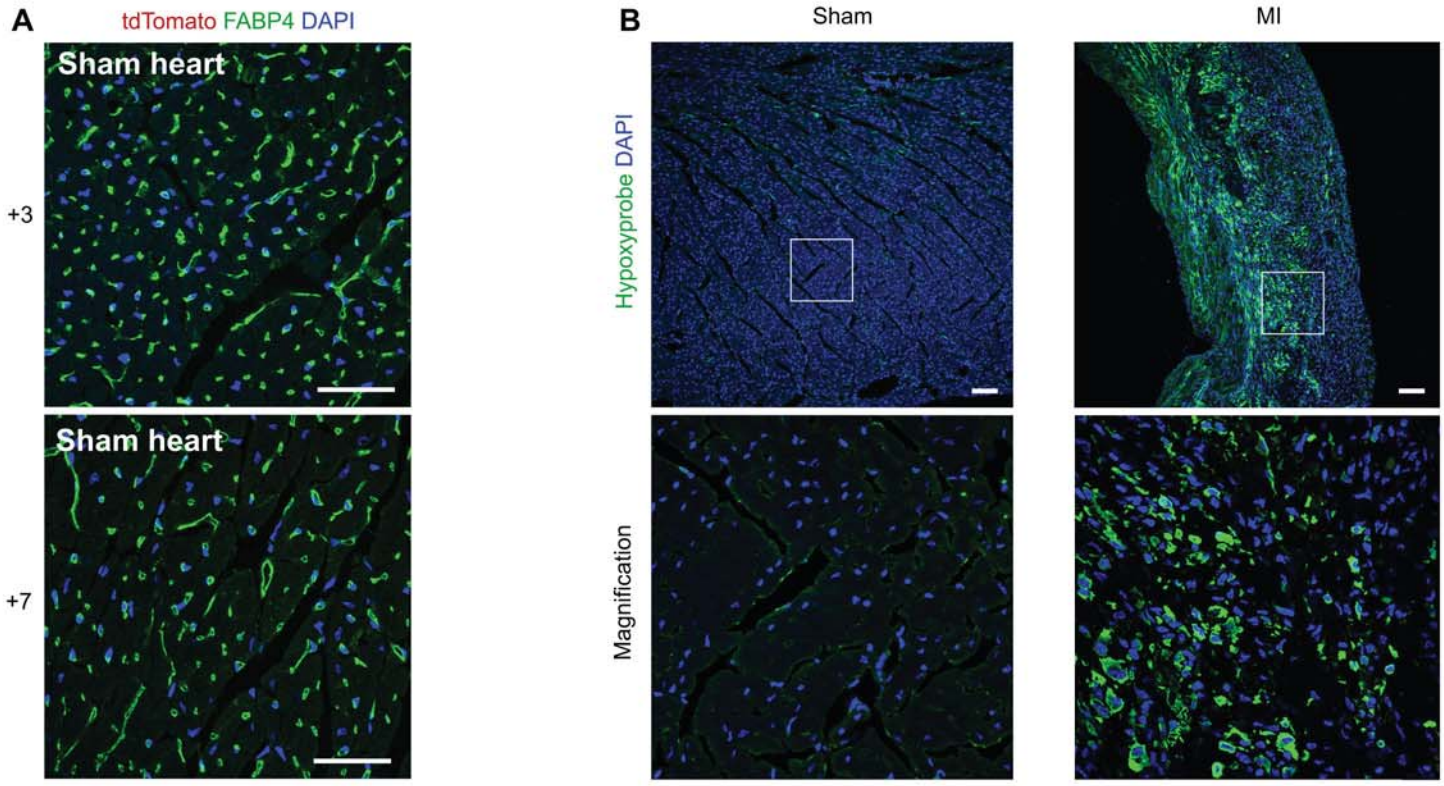

Online Figure XI. Hypoxia in sham and MI heart. A, Immunostaining for tdTomato and FABP4 on sham heart section. Hearts were collected at 3 or 7 days after transplantation of tdTomato+ endocardial cells. **B**, Immunostaining for Hypoxyprobe shows hypoxia in MI but not sham myocardium. Each figure is representative of 5 individual samples.

*** Long In Vivo Checklist**

Circulation Research - Preclinical Animal Testing: A detailed checklist has been developed as a prerequisite for every publication involving preclinical studies of experimental treatments in animals. ***Checklist items must be clearly presented in the manuscript, and if an item is not adhered to, an explanation should be provided.*** *If this information (checklist items and/or explanations) cannot be included in the main manuscript because of space limitations, please include it in an online supplement. If the manuscript is accepted, this checklist will be published as an online supplement. See the explanatory editorial for further information.*

This study involves testing of therapeutic or diagnostic agent in animal models:
Yes

Study Design

The experimental group(s) have been clearly defined in the article, including number of animals in each experimental arm of the study.	Yes
An overall study timeline is provided.	N/A
The protocol was prospectively written	Yes
The primary and secondary endpoints are specified	N/A
For primary endpoints, a description is provided as to how the type I error multiplicity issue was addressed (e.g., correction for multiple comparisons was or was not used and why). (Note: correction for multiple comparisons is not necessary if the study was exploratory or hypothesis-generating in nature).	N/A
A description of the control group is provided including whether it matched the treated groups.	No

Inclusion and Exclusion criteria

Inclusion and exclusion criteria for enrollment into the study were defined and are reported in the manuscript.	Yes
These criteria were set *a priori* (before commencing the study).	Yes

Randomization

Animals were randomly assigned to the experimental groups. If random assignment was not used, adequate explanation has been provided.	Yes
Type and methods of randomization have been described.	Yes
Allocation concealment was used.	Yes
Methods used for allocation concealment have been reported.	Yes

Blinding

Blinding procedures with regard to masking of group/treatment assignment from the experimenter were used and are described. The rationale for nonblinding of the experimenter has been provided, if such was not performed.	Yes
Blinding procedures with regard to masking of group assignment during outcome assessment were used and are described.	Yes
If blinding was not performed, the rationale for nonblinding of the person(s) analyzing outcome has been provided.	N/A

Sample size and power calculations

Formal sample size and power calculations were conducted before commencing the study based on *a priori* determined outcome(s) and treatment effect(s), and the data are reported.	Yes
If formal sample size and power calculation was not conducted, a rationale has been provided.	N/A

Data Reporting

Baseline characteristics (species, sex, age, strain, chow, bedding, and source) of animals are reported.	Yes
The number of animals in each group that were randomized, tested, and excluded and that died is reported. If the experimentation involves repeated measurements, the number of animals assessed at each time point is provided is provided for all experimental groups.	Yes
Baseline data on assessed outcome(s) for all experimental groups are reported.	Yes
Details on important adverse events and death of animals during the course of the experiment are reported for all experimental groups.	Yes
Numeric data on outcomes are provided in the text or in a tabular format in the main article or as supplementary tables, in addition to the figures.	Yes
To the extent possible, data are reported as dot plots as opposed to bar graphs, especially for small sample size groups.	N/A
In the online Supplemental Material, methods are described in sufficient detail to enable full replication of the study.	Yes

Statistical methods

The statistical methods used for each data set are described.	Yes
For each statistical test, the effect size with its standard error and *P* value is presented. Authors are encouraged to provide 95% confidence intervals for important comparisons.	Yes
Central tendency and dispersion of the data are examined, particularly for small data sets.	Yes
Nonparametric tests are used for data that are not normally distributed.	N/A
Two-sided *P* values are used.	Yes
In studies that are not exploratory or hypothesis-generating in nature, corrections for multiple hypotheses testing and multiple comparisons are performed.	N/A
In "negative" studies or null findings, the probability of a type II error is reported.	N/A

Experimental details, ethics, and funding statements

Details on experimentation including formulation and dosage of therapeutic agent, site and route of administration, use of anesthesia and analgesia, temperature control during experimentation, and postprocedural monitoring are described.	Yes
Both male and female animals have been used. If not, the reason/justification is provided.	No
Statements on approval by ethics boards and ethical conduct of studies are provided.	Yes
Statements on funding and conflicts of interests are provided.	Yes

---

Date completed: 01/22/2018 09:19:24
User pid: 101754